



저작자표시-변경금지 2.0 대한민국

이용자는 아래의 조건을 따르는 경우에 한하여 자유롭게

- 이 저작물을 복제, 배포, 전송, 전시, 공연 및 방송할 수 있습니다.
- 이 저작물을 영리 목적으로 이용할 수 있습니다.

다음과 같은 조건을 따라야 합니다:



저작자표시. 귀하는 원저작자를 표시하여야 합니다.



변경금지. 귀하는 이 저작물을 개작, 변형 또는 가공할 수 없습니다.

- 귀하는, 이 저작물의 재이용이나 배포의 경우, 이 저작물에 적용된 이용허락조건을 명확하게 나타내어야 합니다.
- 저작권자로부터 별도의 허가를 받으면 이러한 조건들은 적용되지 않습니다.

저작권법에 따른 이용자의 권리는 위의 내용에 의하여 영향을 받지 않습니다.

이것은 [이용허락규약\(Legal Code\)](#)을 이해하기 쉽게 요약한 것입니다.

[Disclaimer](#)

공학박사 학위논문

**The study on the epitaxial growth of
gallium nitride by HVPE**

2014년 6월

서울대학교 대학원

재료공학부

이 문 상

The study on the epitaxial growth of gallium nitride by HVPE

A DISSERTATION SUBMITTED TO
DEPARTMENT OF MATERIALS SCIENCE AND ENGINEERING
SEOUL NATIONAL UNIVERSITY

FOR THE DEGREE OF
DOCTOR OF PHILOSOPHY

Moonsang Lee

June 2012

Abstract

Gallium nitride(GaN) has been viewed as the most promising materials for opto-electronic devices emitting from blue to ultra violet wavelength as well as high power, and frequency electronic devices owing to its physical properties such as wide and direct bandgap (3.4 eV), high thermal conductivity, and high breakdown voltage.¹ Regardless of unlimited potential for GaN, owing to the lack of native GaN substrates, current GaN substrates, indeed, have been fabricated by the hetero-epitaxial growth technique on foreign substrates such as metal organic chemical vapor deposition (CVD), molecular beam epitaxy (MBE), and hydride vapor phase epitaxy (HVPE). The hetero-epitaxy growth of GaN, however, results in high dislocation density (more than $10^8/\text{cm}^2$) originated from the interface between GaN and foreign substrates, which degrades its optical and electrical properties by the loss of internal quantum efficiency.² As an alternative, the use of freestanding GaN wafers could prevent it. (Via HVPE with high growth rate and relatively high crystal quality, freestanding GaN have been prepared until now.^{3, 4}) There, however, have been a few issues to take it to the real applications. These puzzles are as follows; The first one is the relative high defect densities, primarily in the form of threading dislocations originated from the interface between grown GaN layer and foreign substrates owing to

lattice mismatch and thermal expansion coefficient between GaN and foreign substrate.⁵ Even though the defect density of freestanding GaN is relatively low ($\sim 10^6/\text{cm}^2$), it may not be sufficient for application of power electronic devices, and laser diodes. The second is the size limitation and cost for fabricating freestanding GaN. To get freestanding GaN with low cost and large diameter, the seed substrates with some criterions have to be prepared. The requirements of seed substrates for growing GaN are crystal structure equal to that of GaN, relatively small difference of thermal expansion coefficient and lattice constant for GaN, and low cost. In case of GaAs, the price of GaAs substrate is too high to be used as a substrate to grow freestanding GaN substrates. Also, A sapphire with its current size limitation below 6 inch diameters cannot be a replacement for large-sized GaN substrates. As well, even if sapphire substrate more than 8 inch diameters would be, the bowing of GaN grown from sapphire substrate would be too high to use GaN substrate for commercial. The price of sapphire substrate, of course, will be high.

In this dissertation, I will show the growth of freestanding GaN by various methods in HVPE.

First, we propose a new method to make stress relaxation layers by forming AlN and GaN nano dots on sapphire substrate using NH_3 and HCl treatment. Via this method, a freestanding GaN with 400 μm in thickness and

4 inch in size was obtained. . The value of FWHM in (0 0 0 2) X-ray rocking curve of a thick GaN was 220 arcsec. After lift-off of sapphire substrate, FWHM obtained for (0 0 0 2) reflection were 123 arcsec, which the bowing of wafer was changed from convex to concave, implying the tensile stress. etch pit density about $5 \times 10^6/\text{cm}^2$ confirmed its high crystal quality. Photoluminescence spectroscopy represent the optical property of freestanding GaN where the band edge peak was on 3.393 eV which was moved to red-shift by about 78 meV compared to strain-free bulk GaN, indicating tensile stress in GaN layers.

Next, the homoepitaxial bulk GaN growth with extremely low defect density will be demonstrated. The unique approach was used for the growth of GaN on GaN substrates where substrates were pre-treated by HCl and H_3PO_4 acid solution every 1 mm thickness and sequentially proceeded homoepitaxial growth. We named for it the pit-assisted growth method. The etch pits generated by intentional pit formation, is composed of three kinds of types: α -type etch pit - an inverse-truncated hexagonal pit, the β type one - an inverse-hexagonal pyramid, and the last γ type one - a trapezoidal type. Each etch pit types are related to the screw, edge, and mixed dislocation, respectively. Similarly to the results from other freestanding GaN, most of etch pits consists of β type etch pit, originating from the edge dislocations. This means that screw dislocations are readily annihilated by increasing the

thickness of GaN.

By applying it, bulk GaN with 5 mm in thickness, and 3 inch in size, respectively represented the etch pit density with $3 \times 10^2/\text{cm}^2$.

In last part, it will present how to fabricate freestanding GaN from Si substrate. Until now, freestanding GaN wafers could not be obtained from Si substrate owing to various issues such as tensile stress evolution, and meltback effect. We, however, can fabricate the freestanding GaN wafers from Si substrate via a novel growth concept, namely it-situ removal of substrate. To prevent the formation of cracks in the GaN layer during cooling, Si substrate was removed at high temperature, which successfully suppressed the tensile stress evolution in GaN. By using it, we demonstrated the freestanding GaN with 2 inch in diameter and 400 μm in thickness grown from Si substrate by HVPE. The freestanding GaN exhibited high-quality with the values of FWHM of 65 arcsec in (0002) x-ray rocking curve and etch pit density of less than $1 \times 10^6/\text{cm}^2$. It may be possible to fabricate high-quality freestanding GaN substrates of over 8 inches in diameter using this method.

Key words: GaN, freestanding GaN, HVPE, dislocations, stress relaxation layer, nano dots, etch pit, photoluminescence, bulk GaN, pit-assisted growth, in-situ removal

Student number: 2011-30937

Table of contents

Abstract	i
List of tables	x
List of figures	xi
CHAPTER 1. The need for freestanding GaN	1
1.1. Introduction	3
1.2. Why freestanding GaN	7
1.3. The properties of GaN	11
1.4. HVPE system for GaN growth	15
1.5. Summary	17
References	19
CHAPTER 2. A thick GaN on sapphire substrate	22
2.1. Introduction	24
2.2. Experimental details	26
2.3. Results and discussion	27
2.3.1. AlN and GaN dot formation for stress relaxation layer	27
2.3.2. Numerical analysis of gas flow rate in HVPE reactor	39

2.3.3. Properties of GaN/sapphire	44
2.4. Summary and conclusions	49
References	51

CHAPTER 3. Bulk GaN growth on GaN substrate with extremely low defect density 54

3.1. Introduction	56
3.2. Experimental details	57
3.3. Results and discussion	59
3.3.1. Pit formation revealed by HCl gas and H ₃ PO ₄ acid solution	60
3.3.2. Pit annihilation	63
3.3.3. Mechanism of dislocation reduction	66
3.3.4. Suppression of polycrystalline GaN generation	69
3.3.5. Suppression of micro cracks in bulk GaN	71
3.3.6. Properties of bulk GaN with 5 mm in thickness	73
3.4. Summary and conclusions	79
References	82

CHAPTER 4. Freestanding GaN on Si substrate using in situ

removal of substrate	85
4.1. Introduction	87
4.2. Experimental details	89
4.3. Results and discussion	91
4.3.1. Design of HVPE reactor for in situ removal of Si substrate	91
4.3.2. Numerical analysis for in situ removal of Si substrate	93
4.3.3. Effects on gas flow rate and susceptor design for the etch of Si substrate	101
4.3.4 Meltback effect as a function of MOCVD buffer layer	106
4.3.5. The properties of freestanding GaN grown from Si substrate	108
4.4. Summary and conclusions	115
References	116
 CHAPTER 5. Summary and conclusions	 120
 Abstract (in Korean)	 125

Acknowledgement (in Korean)	127
-----------------------------------	-----

List of tables

CHAPTER 1

Table 1-1. The properties of substrates for GaN epitaxy

Table 1-2. The properties of GaN

CHAPTER 2

Table 2-1. Residual strain of freestanding GaN

List of figures

CHAPTER 1

Figure 1-1. The illustration of performance of LED using freestanding GaN wafers (a) LED efficiency vs substrate (b) light output with forward current vs LED type and substrates

Figure 1-2. The on-resistance versus breakdown voltage with various materials such as Si, SiC, and GaN

Figure 1-3. Bandgap energy versus lattice constant for various semiconductors including the wide-bandgap materials SiC and GaN with its alloys

Figure 1-4. The crystal structure of wurtzite GaN

Figure 1-5. Schematic diagram of HVPE

Figure 1-6. Schematics of laser lift-off process in GaN

CHAPTER 2

Figure 2-1. Schematic diagram of AlN and GaN dot formation.

Figure 2-2. Plan view SEM images of (a) AlN nano dots and (b) GaN nano dots formed on Al₂O₃ substrate.

Figure 2-3. EDS analysis of GaN nano dots based on AlN nano dots taken by plan view SEM.

Figure 2-4. The average size of GaN nano dots as a function of pretreatment temperature.

Figure 2-5. Atomic force microscopy images of GaN nano dots formed on Al₂O₃ substrates at various pretreatment temperatures. The scale bar on each image is 1 μm .

Figure 2-6. The optical microscopy image of growing GaN with buffer layers in thickness of (a) 20 μm and (b) 70 μm formed by GaN nano dots on Al₂O₃ substrates.

Figure 2-7. The dependence of critical thickness of growing GaN layers as a function of the average size of GaN nano dots.

Figure 2-8. The FWHM of (0 0 0 1) X-ray rocking curve on a 300 μm -thick GaN as a function of HCl and NH_3 flow rate during pretreatment stage.

Figure 2-9. The schematics of (a) our HVPE system and its (a) one gas nozzle geometry and (b) three gas nozzles of tripod shape

Figure 2-10. The mass fraction of (a) NH_3 and (b) GaCl gases as a function of distance between gas inlets and wafer. Gas flow rate of GaCl, NH_3 is 400 sccm, and 4800 sccm, respectively. Pressure in reactor is atmosphere, and temperature in reactor is 1000 $^\circ\text{C}$

Figure 2-11. Numerical analysis result of (a) the gas flow from GaCl inlets and plane flow near susceptor

Figure 2-12. A thick GaN on sapphire substrate with 4 inch in diameters and 200 μm in thickness

Figure 2-13. X-ray rocking curve of (a) the thick GaN/sapphire (b)

freestanding GaN after removing sapphire substrate

Figure 2-14. Photoluminescence spectrum of freestanding GaN grown on sapphire substrate at room temperature

CHAPTER 3

Figure 3-1. The procedure of bulk GaN growth by pit-assisted method.

Figure 3-2. The optical microscopy images of (a) pits with various size revealed by HCl and H₃PO₄ etch on freestanding GaN, (b) three types of pits, and (c) the schematics of profiles for three kinds of etch pits.

Figure 3-3. The optical microscopy image of (a) pit shape as a function of V/III ratio after growing 1.2 mm-thick GaN on freestanding GaN with 400 μm (b) cross sectional microscopy image of bulk GaN with 1.2 mm thickness. The interface between growing GaN and seed GaN is easily shown by contrast difference.

Figure 3-4. The optical microscopy image of pit shape.

Figure 3-5. The optical microscopy image of expanded pits on V/III ratio with 37 as a function of growing GaN thickness.

Figure 3-6. Schematic diagram of dislocation reduction mechanism: (a) diagram of growth with hexagonal pits constructed by $\{11\bar{2}2\}$ facets concentrating dislocations at the bottom of the pit; (b) diagram of the dislocation propagation from the surface of the facets to the center of the pit; (c) plan-view of the dislocation propagation route within the hexagonal pit.

Figure 3-7. Cross-sectional optical microscopy image of bulk GaN with 2 mm thickness.

Figure 3-8. Additional HCl flow rate vs polycrystalline GaN in bulk GaN.

Figure 3-9. V/III ratio vs polycrystalline GaN in bulk GaN.

Figure 3-10. Experiment condition of bulk GaN and schematics for micro crack..

Figure 3-11. A photograph of bulk GaN with 5 mm thickness and 3 inch diameters grown by pit-assisted growth.

Figure 3-12. The optical microscopy images on the surface of bulk GaN.

Figure 3-13. (0 0 02) X-ray rocking curve of bulk GaN with 5 mm in thickness.

Figure 3-14. The optical microscopy image of bulk GaN after dipping in H_3PO_4 acid solution at $200\text{ }^\circ\text{C}$ during 30 min.

Figure 3-15. (a) bulk GaN thickness with varying pit size vs FWHM of (0 0 0 2) X-ray rocking curve, and (b) bulk GaN thickness vs FWHM and EPD.

CHAPTER 4

Figure 4-1. Schematic illustration of the steps for fabrication of a freestanding GaN on a Si substrate using in-situ Si etching.

Figure 4-2. Schematic diagram of (a) HVPE reactor designed to remove Si substrate at high temperature, and (b) susceptor design to remove Si substrate. Si substrates can be removed by HCl gas flowed from backside in susceptor.

Figure 4-3. (a) CTE of Si and GaN along axis vs temperature, and (b)

Schematics of layer structure applied in numerical analysis. The intrinsic stress at growth temperature was substituted by -679, and 20 MPa in MOCVD-uGaN and HVPE-GaN, respectively.

Figure 4-4. (a) The numerical analysis for temperature dependence of stress in a thick GaN layer grown on Si substrate. (b) The numerical analysis for temperature dependence of stress and bowing in GaN grown on Si substrate.

Figure 4-5. (a) Susceptor type used in the etch of Si substrate, and (b) etch rate of Si substrate as a function of susceptor types and gas flow rate.

Figure 4-6. (a) Loading position of a Si substrate on susceptor vs HCl flow rate, and (b) etch rate of a Si substrate.

Figure 4-7. (a) Cross sectional transmission electron microscopy image of the backside on a Si substrate after etching Si substrate in HVPE reactor. (b) EDS data on backside of a Si substrate after growing GaN and then applying in-situ etch of Si substrate in HVPE reactor.

Figure 4-8. MOCVD buffer layer thickness vs bowing of MOCVD buffer

layer/Si templates.

Figure 4-9. (a) Photograph of the freestanding GaN of 400 μm in thickness and with a diameter of about 2 inches. (b) Surface image of the freestanding GaN obtained using an optical microscope. (c) Cross-sectional microscopic image of the freestanding GaN ($\times 400$).

Figure 4-10. (a) Micro Raman scattering spectra of a freestanding GaN wafer and (b) micro Raman intensity profiles for E_2 (high)

Figure 4-11. (a) (0002) X-ray rocking curve of the freestanding GaN. (b) Microscopic image of the freestanding GaN after H_3PO_4 etching at 200 $^\circ\text{C}$ for 30 min.

Figure 4-12. PL spectrum of freestanding GaN at 10 K.

CHAPTER 1.

The need for freestanding GaN

1.1. Introduction

Gallium nitride(GaN) has been viewed as the most promising materials for opto-electronic devices emitting from blue to ultra violet wavelength as well as high power, and frequency electronic devices owing to its physical properties such as wide and direct bandgap (3.4 eV), high thermal conductivity, and high breakdown voltage.¹ Regardless of unlimited potential for GaN, owing to the lack of native GaN substrates, current GaN substrates, indeed, have been fabricated by the hetero-epitaxial growth technique on foreign substrates such as metal organic chemical vapor deposition (CVD), molecular beam epitaxy (MBE), and hydride vapor phase epitaxy (HVPE). The hetero-epitaxy growth of GaN, however, results in high dislocation density (more than $10^8/\text{cm}^2$) originated from the interface between GaN and foreign substrates, which degrades its optical and electrical properties by the loss of internal quantum efficiency.² As an alternative, the use of freestanding GaN wafers could prevent it. (Via HVPE with high growth rate and relatively high crystal quality, freestanding GaN have been prepared until now.^{3, 4}) There, however, have been a few issues to take it to the real applications. These puzzles are as follows; The first one is the defect densities, primarily in the form of threading dislocations originated from the

interface between grown GaN layer and foreign substrates owing to lattice mismatch and thermal expansion coefficient between GaN and foreign substrate.⁵ Even though the defect density of freestanding GaN is relatively low ($\sim 10^6/\text{cm}^2$), it may not be sufficient for application of power electronic devices, and laser diodes. The second is the size limitation and cost for fabricating freestanding GaN. To get freestanding GaN with low cost and large diameter, the seed substrates with some criterions have to be prepared. The requirements of seed substrates for growing GaN are crystal structure equal to that of GaN, relatively small difference of thermal expansion coefficient and lattice constant for GaN, and low cost. The materials satisfied above are on the table 1. The most preferable listed in table 1. are GaAs, and sapphire so far. In case of GaAs, the price of GaAs substrate is too high to be used as a substrate to grow freestanding GaN substrates. Also, A sapphire with its current size limitation below 6 inch diameters cannot be a replacement for large-sized GaN substrates. As well, even if sapphire substrate more than 8 inch diameters would be, the bowing of GaN grown from sapphire substrate would be too high to use GaN substrate for commercial. The price of sapphire substrate, of course, will be high.

Substrates	Lattice parameters, Å		Lattice parameter mismatch, %	Thermal expansion coefficient, ($\times 10^{-6}$ K ⁻¹)	
	a	c		a	c
GaN – wurtzite	3.189	5.18	0	5.59	3.17
AlN – wurtzite	3.112	4.98	2.5	4.2	5.3
6H-SiC – wurtzite	3.08	15.12	3.5	4.2	4.7
Al ₂ O ₃ – wurtzite	4.758	12.991	16.1	7.5	8.4
ZnO – wurtzite	3.21	5.21	1.94	2.9	4.8
LiAlO ₂ – tetragonal	5.1687	6.2679	1.5	7.1	7.5
LiGaO ₂ -orthorhombic	5.402	5.007	0.9	6	7
Si(111) – hexagonal	5.83	--	20.5	4.2	--
GaN – zinc blende	4.53	--	16.57	5.2	--
3C-SiC – diamond	4.36	--	3.9	4.5	--
GaAs – zinc blende	5.65	--	19.87	6.0	--

Table 1-1. The properties of substrates for GaN epitaxy

In this dissertation, I will show the growth of freestanding GaN by various methods in HVPE. In chapter 1, I will describe the inevitable need of freestanding GaN for applications such as light emitting diodes (LED), laser diodes (LD), and power devices, addressing the relation between device performances and substrates. Next, the physical properties of GaN will be summarized. Subsequently, the fundamental thermodynamics and chemistry in HVPE will be characterized to understand GaN growth.

Chapter 2 provides details for the growth of GaN on sapphire substrate with 4 inch diameters in HVPE where AlN and GaN dot nuclei buffer layer acting as stress relaxation buffer layer will be on the pages, and some growth parameters for relatively large sized-GaN growth such as pretreatment, growth temperature, and V/III ratio and their effects on GaN crystal quality, and cracks will be shown.

In chapter 3, the homoepitaxial bulk GaN growth will be demonstrated. For freestanding GaN with extremely low defect density below $10^5/\text{cm}^2$, the unique approach was used for the growth of GaN on GaN substrates where substrates was pre-treated by some chemicals and growth conditions were optimized by controlling ratio of group V and group III, growth temperature to relieve micro and macro cracks by stress evolution and prevent the pit generation and remove existing pits during homoepitaxial GaN growth.

Next, it will be codified as chapter 5, the growth of freestanding GaN on Si substrate. I discuss the limit of the state of the arts of freestanding GaN and new concept, in-situ removal of substrates, to overcome it. Using this technique, we could expect to get freestanding GaN with large size, low fabrication cost, and high crystal quality.

Finally, I will put briefly and present my conclusion in chapter 6. I will make propositions to further research and development for techniques used in this dissertation, including non polar a-plane, r-plane, and semi polar freestanding GaN with large size diameter and high crystal quality. By applying this ways, it may be possible to produce freestanding GaN wafers for improved devices performances all in device types.

1.2. Why freestanding GaN

I briefly put some explanations why freestanding GaN would be inevitable in previous section where hetero-epitaxy growth is essential to grow GaN owing to the absence of native GaN substrate, which results in the generation of threading dislocations². On account of this, GaN-based LEDs experience the decline in their performances by make the fall of internal and external quantum efficiency.^{6, 7} The total efficiency of LEDs is given by

$$\varepsilon \text{ (lm/W)} = \eta_{\text{int}} \times \eta_{\text{ext}} \times \eta_{\text{QD}} \times \eta_{\text{ph}}(\text{T}) \times \eta_{\text{pkg}} \quad (1)$$

where η_{int} is the internal quantum efficiency, η_{ext} is the external quantum efficiency, η_{QD} and $\eta_{\text{ph}}(\text{T})$ is the efficiency by phosphor, and pkg is the efficiency by packaging, respectively. Among these factors, the internal quantum efficiency (IQE) is related to the defect density, internal resistance, composition of quantum well layers, and so on. In particular, the defect density significantly influences on the device performance by making non-radiative recombination center in which recombination between electron and hole is induced into phonon, indicating the loss of internal quantum efficiency. Also, the efficiency droop phenomena, the decrease in external quantum efficiency (EQE) of LEDs with increasing drive current is one of the most significant and challenging issues confronting GaN-based LEDs.⁷

Figure 1-1 illustrates the effects of freestanding GaN wafers to improve the device performance in LEDs. Figure 1-1(a) clearly shows the relation between defect density and internal quantum efficiency in LEDs, indicating dislocations significantly affects the efficiency, i.e., dislocations behave as non-radiative recombination centers leading to the loss of internal quantum efficiency. GaN-based LEDs using freestanding GaN wafers successfully reduce the degradation of internal quantum efficiency originated from the dislocations compared to GaN-based LED on foreign substrates with higher dislocation density. Also, efficiency droop caused by a non-radiative carrier loss mechanism can be prevented by using freestanding GaN wafers as depicted in Fig. 1-1(b). Typically, GaN based-LEDs have a peak efficiency before the efficiency gradually drops where it can suffer more than 40% loss of efficiency from a highest current. Indeed, this is a severe issue for high power LEDs requiring high current to operate. Several proposed models for the origin of efficiency droop phenomena such as dislocations⁸, Auger recombination⁹, and carrier delocalization¹⁰ were discussed. It, however, is controversial whether what is the origin. Despite of the lack of understanding for efficiency droop, it could be overcome by using freestanding GaN.¹¹ Otherwise, the device reliability that has correlation with dislocation density can also be improved if freestanding GaN wafer would be applied.

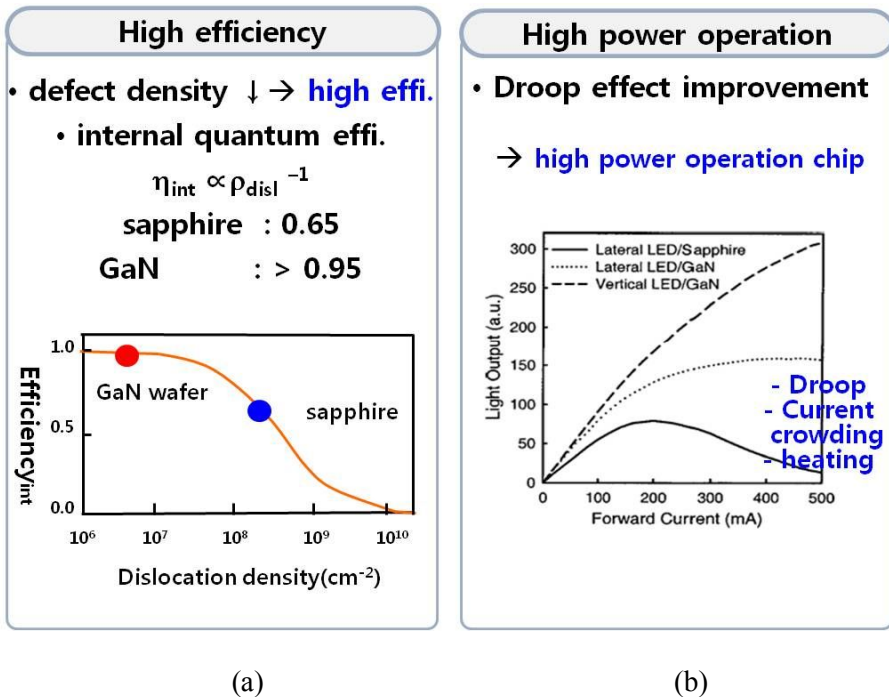


Figure 1-1. The illustration of performance of LED using freestanding GaN wafers (a) LED efficiency vs substrate (b) light output with forward current vs LED type and substrates

At present, the high frequency and high power devices is dependent upon the wide-bandgap materials. High power devices and switching devices demonstrate performance relying on threading dislocation density. Reduced dislocation density results in the decreased gate leakage current, implying better device performance. As well, by applying for freestanding GaN wafer to power devices, the vertical device structure can be fabricated, which enables small chip size, easy wiring, higher breakdown voltage, current

collapse-free operation, and higher current conduction.¹²⁻¹⁴ Figure 1-2 illustrates on-resistance versus breakdown voltage for GaN FET and diodes. Improved GaN device performance compared to SiC and Si is expected to extend to devices such as HFETs and MOSFETs enabling to be used as the transistor in converter and inverter circuits. Higher channel mobilities for GaN MOSFETs have been demonstrated and are expected to even further increase with decreasing defect density. As a result, the channel component of the on-resistance is expected to be even lower for GaN MOSFETs, and the drift component to be lower owing to the higher breakdown electric field. Thus, GaN MOSFET with even higher efficiency switching performance can be considered by lower switching losses and power consumption when compared to SiC and Si materials.¹⁵⁻¹⁷

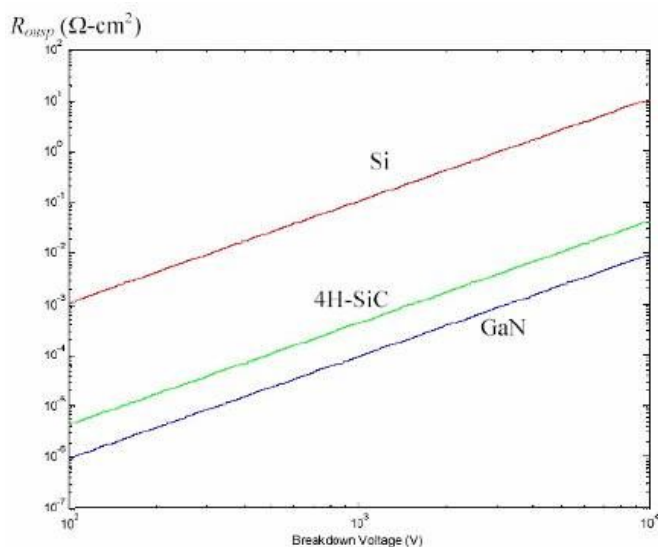


Figure 1-2. The on-resistance versus breakdown voltage with various materials such as Si, SiC, and GaN

1.3. The properties of GaN¹⁸

The physical properties of GaN make it an attractive semiconductor for many electronic and optoelectronic devices. The electrical property of GaN with wide and direct energy band gap makes it suitable for various applications such as LEDs, lasers diodes, and detectors. As well, the properties of the wide energy band gap and good thermal stability of GaN is the essential for high-temperature (HT) and high power electronics. Gallium nitride can represent a wide range of energy bandgaps (1.9 - 6.2 eV) by forming solid solutions with AlN and InN, which is critical to be used as emitters with specific wavelengths, and for creating heterojunctions with potential barriers into the device structures (Note that the wavelength of GaN-based materials correspond to the range from red to deep UV as depicted in Fig 1-3).

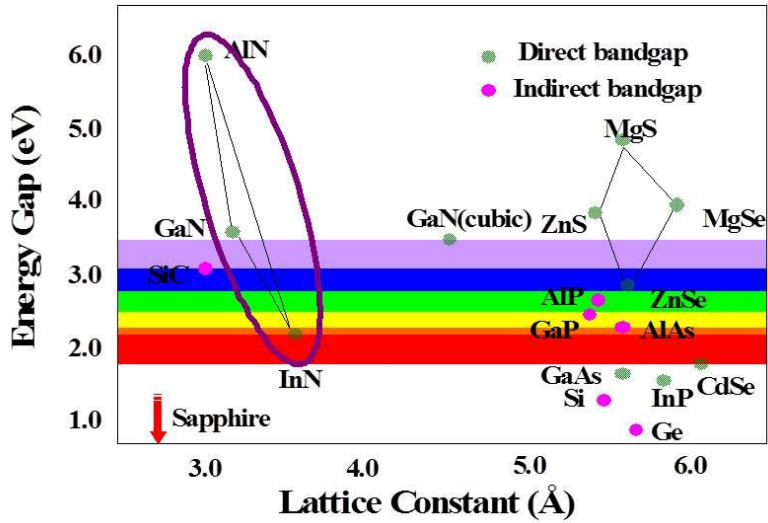


Figure 1-3. Bandgap energy versus lattice constant for various semiconductors including the wide-bandgap materials SiC and GaN with its alloys

In addition, high thermal conductivity make it easy way for GaN-based devices by facilitating heat dissipation in them compared to silicon and gallium arsenide. Both n- and p-type conductivities are possible in GaN. Because the group III nitrides do not have inversion center and have significantly ionic chemical bonding, they have strong piezoelectricity, experiencing spontaneous polarization^{19, 20}. These effects can be advantageously employed, to increase the sheet carrier concentration in heterostructure transistor²¹. The physical properties of gallium nitride is

shown in Table 1-2. The thermal expansion coefficients of semiconductors including GaN depend on the temperature, and here only % changes in lattice constants for certain temperature range are listed in this paper. Gallium nitride with the space group of $P6_3mc$ (no. 186), indicating a wurtzite structure forms alternating biatomic close-packed (0 0 01) planes of Ga and N pairs stacked in an ABABAB sequence. Atoms in the first and third layers are directly aligned with each other.

Property	Value
Energy band gap (eV) (300 K)	3.44
Maximum electron mobility ($\text{cm}^2/\text{V s}$)	
300 K	1350
77 K	19200
Maximum hole mobility (300 K) ($\text{cm}^2/\text{V s}$)	13
Controlled doping range (cm^{-3})	
n-type	$10^{16} \sim 4 \times 10^{20}$
p-type	$10^{16} \sim 6 \times 10^{18}$
Melting point (K)	> 2573 (at 60 kbar)
Lattice constants (300 K)	

a (nm)	0.318843
c (nm)	0.518524
Percentage change in lattice constants (300–1400 K)	$\Delta a/a_0$ 0.5749, $\Delta c/c_0$ 0.5032
Thermal conductivity (300 K) (W/cm K)	2.1
Heat capacity (300 K) (J/mol K)	35.3
Modulus of elasticity (GPa)	210 ± 23
Hardness (nanoindentation, 300 K) (GPa)	15.5 ± 0.9
Hardness (Knoop, 300 K) (GPa)	10.8
Yield strength (1000 K) (MPa)	100

Table 1-2. The properties of GaN

Figure 1-4 shows the schematics for the crystal structure of wurtzite GaN, where the green and brown circles represent gallium and nitrogen atoms, respectively. The close-packed planes are the (0 0 0 1) planes. The group III nitrides lack an inversion plane perpendicular to the c -axis, thus, crystals surfaces have either a group III element (Al, Ga, or In) polarity (designated (0 0 01) or (0 0 0 1)A) or a N-polarity (designated (0 0 0 $\bar{1}$) or (0

0 0 1)B). An excellent review on crystal polarity is given by Hellman²².

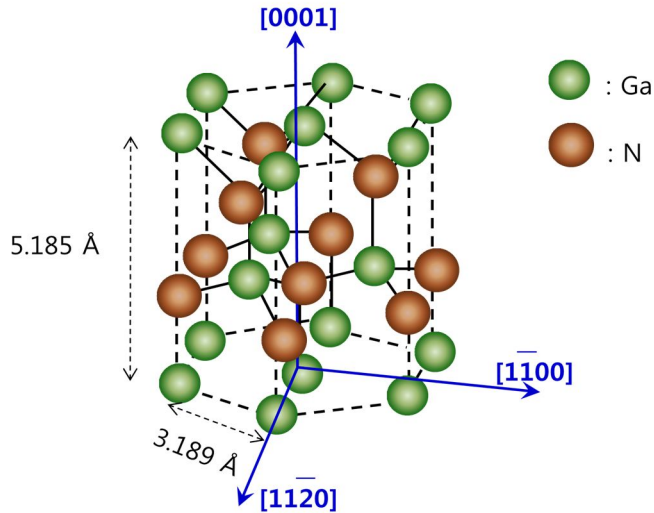


Figure 1-4. The crystal structure of wurtzite GaN

1.4. HVPE system for GaN growth

Hydride vapor phase epitaxy (HVPE) is the most successful epitaxial growth technique since early stage of the group III nitrides owing to high growth rate, and relatively high crystal quality.²³ In particular, HVPE has significantly received attention for commercial freestanding GaN. In this section, we will take a glance at thermodynamic, theoretical study and HVPE system about HVPE.

HVPE is a kind of chemical vapor phase deposition method. In case of

HVPE for GaN, the source materials consist of a kind of Ga chloride and NH₃. The gallium monochloride (GaCl) precursor, especially is used as a Ga precursor, which is synthesized within the reactor by the reaction of hydrochloric acid (HCl) with liquid Ga metal at temperatures between 700 °C and 900 °C. The GaCl is then transported to the foreign substrate, e.g. sapphire, Si, GaAs, and SiC, where it reacts with ammonia (NH₃) at 1000 °C-1100 °C to form GaN as shown in Fig. 1-5.

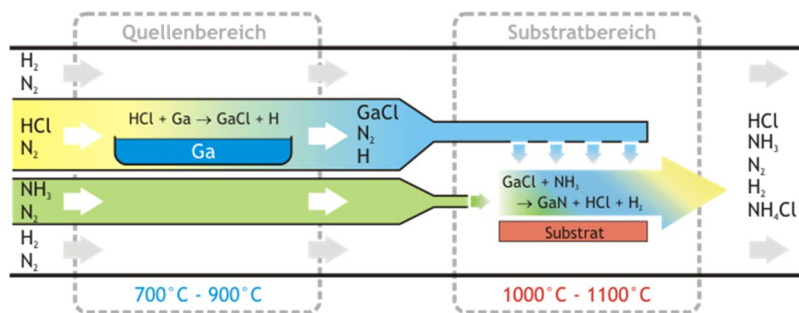


Figure 1-5. Schematic diagram of HVPE

As grown GaN with the foreign substrate after the growth process have to be treated by laser lift-off process using Nd:YAG laser with wavelength of 325 nm to take off the foreign substrates as illustrated in Fig. 1-6.

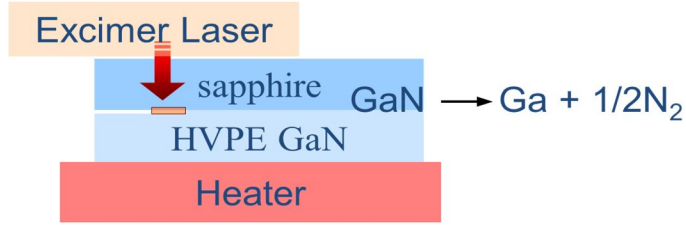
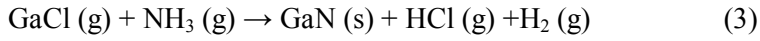


Figure 1-6. Schematics of laser lift-off process in GaN

The GaN growth process in reactor can be explained as follows²⁴



Typically, HVPE has high growth rate over 100 $\mu\text{m/hr}$, thus is the most commonly used method to make freestanding GaN with thick, and low defect density GaN.

1.5. Summary

In a nutshell, GaN has been regarded as one of the most fascinating material to apply for opto-electric and electronic devices. In particular, the use of freestanding GaN may be predestined to prevent negative effects, e. g. efficiency droop, and high on-resistance, in GaN-based devices. Despite of various advantages for freestanding GaN, there has long been known that

difficult issues such as cost, and size limitation to block the readily application for devices based on freestanding GaN exist. In this dissertation, , I will show the possibility for widespread use of freestanding GaN by suggesting various method to overcome them.

References

- [1] S. Nakamura, M. Senoh, and T. Mukai, 1993, *Appl. Phys. Lett.* **62**, 2390
- [2] I. Ma'rtıl, E. Redondo, and A. Ojeda, 1997, *J. Appl. Phys.*, **81**, 2442
- [3] H. Amano, N. Sawaki, I. Akasaki, and Y. Toyoda, 1986, *Appl. Phys. Lett.* **48**, 353
- [4] H. Larsson, D. Gogova, A. Kasic, R. Yakimova, B. Monemar, C. R. Miskys, and M. Stutzmann, 2003, *Phys. Stat. sol.(c)*. **0**, 1985
- [4] M. K. Kelly, R. P. Vaudo, V. M. Phanse, L. Go'rgens, O. Ambacher, and M. Stutzmann, 1999, *Jpn. J. Appl. Phys.* **38**, L217
- [5] I. Ma'rtıl, E. Redondo, and A. Ojeda, 1997, *J. Appl. Phys.*, **81**, 2442
- [6] J. Piprek, 2010, *Phys. Status Solidi A* **207**, 2217
- [7] M. F. Schubert, J. Xu, Q. Dai, F. W. Mont, J. K. Kim, and E. F. Schubert, 2009, *Appl. Phys. Lett.* **94**, 081114
- [8] Q. Dai, Q. Shan, J. Cho, E. F. Schubert, M. H. Crawford, D.

- D. Koleske, M.-H. Kim, and Y. Park, 2011, *Appl. Phys. Lett.* **98**, 033506
- [9] B. Pasenow, S. W. Koch, J. Hader, J. V. Moloney, M. Sabathil, N. Linder, and S. Lutgen, 2009, *Phys. Status Solidi C* **6**, S864
- [10] M. F. Schubert and E. F. Schubert, 2010, *Appl. Phys. Lett.* **96**, 131102
- [11] B. Monemar and B. E. Semelius, 2007, *Appl. Phys. Lett.* **91**, 181103
- [12] J. Kuzm'k, 2001, *IEEE Electron Device Lett.* **22**, 510
- [13] J. Kuzm'k, 2002, *Semicond. Sci. Technol.* **7**, 540
- [14] W. Huang, T. Khan, and T. P. Chow, 2006, *IEEE Electron Device Lett.* **27**, 796
- [15] T. Uesugi, 2006, *R&D Rev. Toyota CRDL.* **35**, 1
- [16] H. Ueda, M. Sugimoto, T. Uesugi, and T. Kachi, 2006, *CS MANTECH Conf.* 24
- [17] S. J. Pearton and F. Ren, 2000, *Adv. Mater.* **12**, 1571
- [18] L. Liu, and J. H. Edgar, 2002, *Materials Science and Engineering: R: Reports* **37**, 2002

- [19] E.T. Yu, X.Z. Dang, P.M. Asbeck, S.S. Lau, G.J. Sullivan, and M. Andre, 1999, *J. Vac. Sci. Technol. B.* **17**, 1742
- [20] O. Ambacher, R. Dimitrov, M. Suttzmann, B.E. Foutz, M.J. Murphy, J.A. Smart, J.R. Shealy, N.G. Weimann, K. Chu, M. Chumbes, B. Green, A.J. Sierakowski, W.J. Schaff, and L.F. Eastman, 1999 *Phys. Stat. Sol. (b)* **216**, 381
- [21] R. Dimitrov, M. Murphy, J. Smart, W. Schaff, J.R. Sealy, L.F. Eastman, O. Ambacher, and M. Stutzmann, 2000, *J. Appl. Phys.* **87**, 3375
- [22] E.S. Hellman, 1998, *MRS Internet J. Nitride Semicond. Res.* **3**, 11
- [23] H. P. Maruska and J. J. Tietjen, 1969, *Appl. Phys. Lett.* **15**, 327
- [24] V. S. Ban, 1972, *J. Electrochem. Soc.* **119**, 761

CHAPTER 2.

Freestanding GaN on sapphire substrate

2.1. Introduction

GaN is one of the most promising candidates for optoelectronic devices. Since starting the study on GaN, One of the major restrictions for high-quality GaN growth is the lack of a suitable large-area lattice-matched substrate, although attempts to epitaxially grow III–V nitrides on sapphire have been made using metalorganic chemical vapour deposition (MOCVD), molecular beam epitaxy, and hydride vapor phase epitaxy (HVPE).¹⁻³ Despite of many difficulties, it becomes commercially possible to grow a thick GaN on various materials such as sapphire, GaAs, and SiC in HVPE. Among these things, a sapphire (α -Al₂O₃) is widely used as the most common substrates for the growth of GaN owing to its cost, and high stability in high temperature. The hetero-epitaxy growth of GaN, however, results in stress and high defect density resulting from thermal expansion coefficient and lattice mismatch. To overcome these, it is well known buffer layers are grown via materials such as low temperature GaN, and AlN.^{4, 5} In addition, various techniques used as buffer layers, e. g. patterned substrates and epitaxial lateral growth (ELOG) method, have been applied to reduce stress and dislocation density in grown GaN layers.⁶⁻⁸ Despite of these successful studies, freestanding GaN over 2 inch diameters have not been supplied due to insufficient buffer layer function and cost problem.

In this chapter, we propose the simple way to control stress in GaN by forming AlN and GaN nano dots as seed of buffer layer on Al₂O₃ substrate with 4 inch diameters, which make it possible grow freestanding GaN with 4 inch diameters. Moreover, the mechanism for GaN nano dots formation and effects for stress relaxation layers will be studied by evaluating the structural properties of a freestanding GaN grown on Al₂O₃ substrate with 4 inch diameters. A numerical analysis of gas stream in HVPE designed to make freestanding GaN with high crystal quality and crack-free over 4 inch diameters also will be added.

2.2. Experimental details

The thick GaN layers were grown on 4 inch (0 0 0 1) Al_2O_3 substrates in a vertical hot wall HVPE reactor at atmospheric pressure where the carrier gases and precursors are delivered from the top to bottom. Before GaN deposition, special surface treatments on Al_2O_3 substrates were employed at 980 - 1030 °C, i. e. HCl and NH_3 gases were directly incorporated into Al_2O_3 substrate to form AlN and GaN nano dot buffer layer, implying no reaction between active gas and liquid Ga metal as a source of III family material for GaN formation. After surface treatment of Al_2O_3 substrates by HCl and NH_3 gases, the temperature of growth zone was increased in presence of N_2 to 1080 °C to grow GaN. To apply it, HCl was reacted with liquid Ga to form GaCl gas which was transported to the growth zone kept at 1080 °C where it was directly reacted with NH_3 , resulting in GaN deposition. Nitrogen gas was used as a carrier gas. The growth rate was 100 $\mu\text{m/hr}$, and V/III ratio was varied in range of 20–35 with constant GaCl flow rate.

The thick GaN films were separated from Al_2O_3 substrates using a KrF excimer laser (50 Hz, 20 ns). Laser processing was performed in air. The energy density of the incident beam was varied between 0.2-0.3 J/cm^2 . The GaN/ Al_2O_3 during the laser processing was heated up to below the

decomposition temperature of GaN to reduce the bowing-induced fracture formed.^{9, 10}

Consequently, freestanding GaN substrates with 4 inch diameters were mechanically polished and dry-etched on the Ga face to obtain a smooth epi-ready surface.

Double crystal X-ray diffraction, optical microscopy, scanning electron microscopy (SEM), and transmission electron microscopy (TEM) were employed to evaluate the structural properties. The photoluminescence (PL) of the samples was excited using a He-Cd laser with a wavelength of 325 nm. The AFM measurements were performed with a Veeco Dimension 3100 SPM system to analyze the surface morphology.

2.3. Results and discussion

2.3.1. AlN and GaN dot formation for stress relaxation layer

Figure 2-1 illustrates the schematic diagram of AlN nano and GaN nano dot formation. AlN nano dots were formed on Al₂O₃ substrates as seeds of GaN dots, and subsequently GaN dots could be grown on the AlN nano dots. In order to form AlN nano dots on a surface of a Al₂O₃ substrate, HCl and NH₃ gas were simultaneously introduced into a HVPE reactor. Because the surface of the Al₂O₃ substrates is terminated by oxygen dangling bonds, some

oxygen may be removed by HCl, and then the vacancies (originally occupied by the removed oxygen) may be filled by nitrogen thermally decomposed from NH_3 . AlN nano dots were randomly formed on the surface of the Al_2O_3 substrate depending on an oxygen substitution process. Thereafter, GaN nano dots are formed on AlN nano dots.

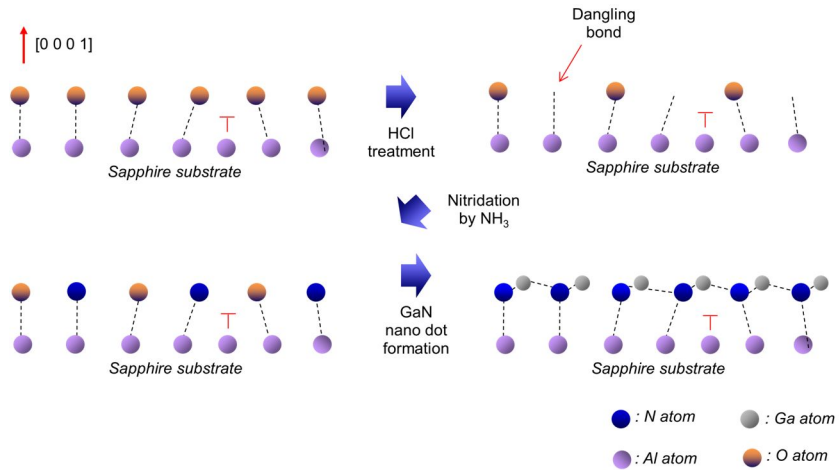


Figure 2-1. Schematic diagram of AlN and GaN dot formation

Figure 2-2 depicts the scanning electron microscope (SEM) image of AlN and GaN nanodots on a Al_2O_3 substrate. The AlN nano dots were formed randomly/uniformly on a sapphire substrate. The average size and density of

AlN nano dots were determined by various growth parameters including, for example, an amount/ (flow rate \times time period) of NH_3 and HCl and/or a surface treatment temperature of the sapphire substrate. As an example, AlN nano dots with diameters of 10 nm and density of $1.5 \times 10^{10}/\text{cm}^2$ could be formed using a 3000 sccm flow rate of NH_3 and a 200 sccm flow rate of HCl , at a sapphire substrate temperature of about 980°C ., for about 5 minutes. The average size of AlN nano dots could be controlled in the range from about a few nm to about a few hundred nm. As expected easily, the AlN nano dots may be part of (e.g., inside) the GaN dots. Energy dispersive X-ray spectroscopy (EDS) analysis shows the component of AlN/GaN dots formed by HCl and NH_3 gases on Al_2O_3 substrates as illustrated in Fig 2-3. The atomic weight percentage for composition of Ga, Al, and N in the absence area of AlN/GaN nano dots is nearly zero, 24.47 %, and 20.57 %, respectively. In the area with nano dots, the atomic weight percentage for composition of Ga, Al, and N is 5%, 27.74%, and 22.24%, indicating GaN nano dots are based on AlN nano dots.

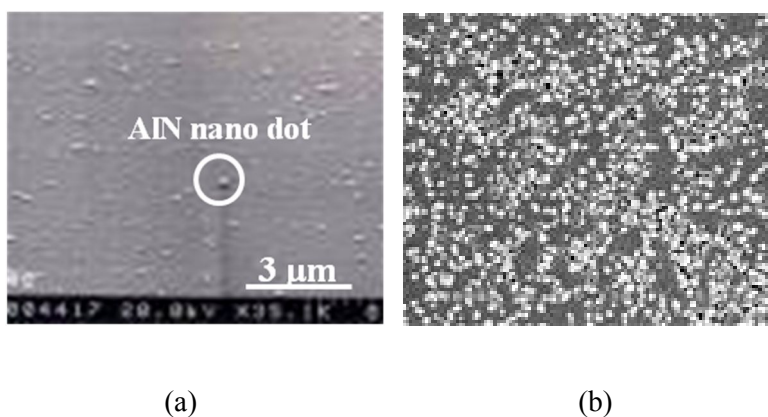


Figure 2-2. Plan view SEM images of (a) AlN nano dots and (b) GaN nano dots formed on Al₂O₃ substrate.

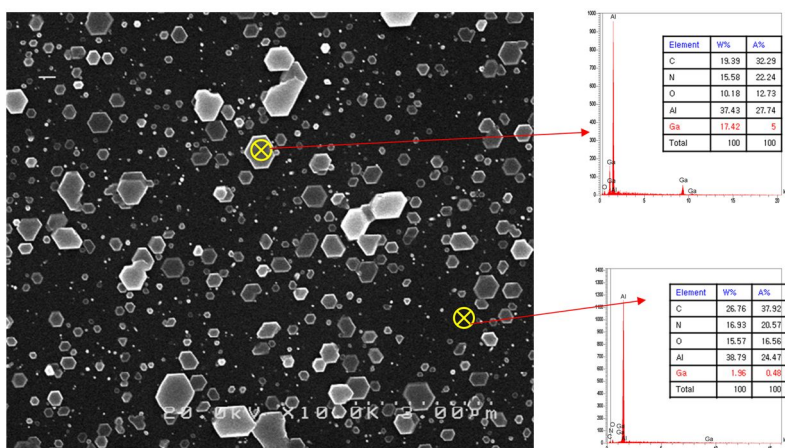


Figure 2-3. EDS analysis of GaN nano dots based on AlN nano dots taken by plan view SEM

Likewise, the average size and density of GaN nano dots are a function of growth parameters such as surface treatment temperature, an amount of NH_3 and HCl , including the average size of AlN nano dots as detailed in Fig. 2-4. The average size of GaN nano dots is increased with increasing pretreatment (surface treatment) temperature. On the other hand, the density of GaN nano dots is decreased with increment of pretreatment temperature.

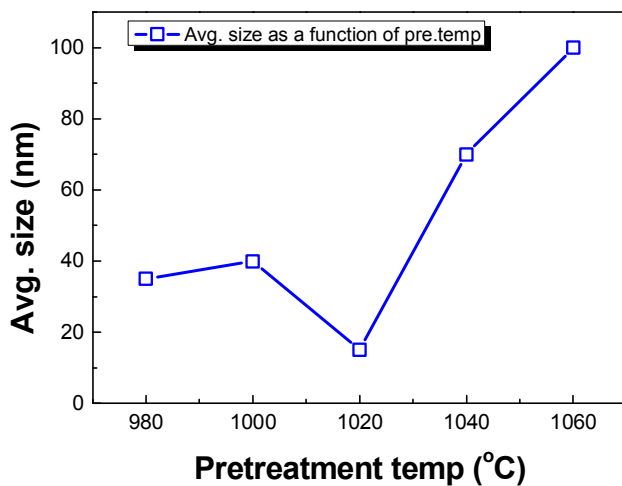
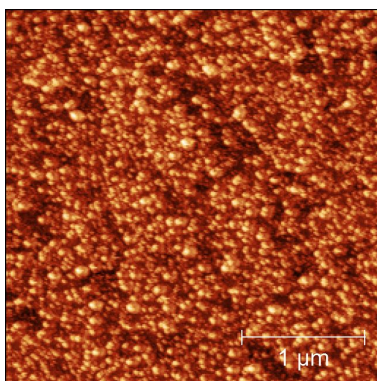


Figure 2-4. The average size of GaN nano dots as a function of pretreatment temperature.

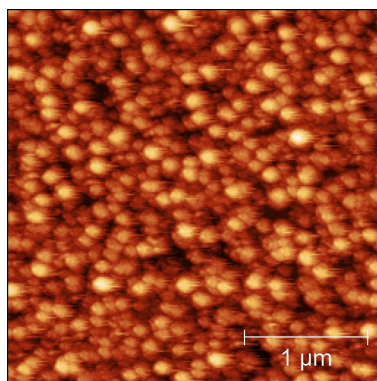
The higher pretreatment temperature, the higher reactivity Al_2O_3 by

active gases such as HCl and NH₃ gas, which results in the higher nucleation sites for AlN nano dot formation from which GaN nano dots can easily coalesce each others. Consequently, the average size and density of GaN nano dots remains bigger and lower in high pretreatment temperature compared to those in low pretreatment temperature. We can consider it vice versa in case of AlN/GaN nano dot formation in low pretreatment temperature.

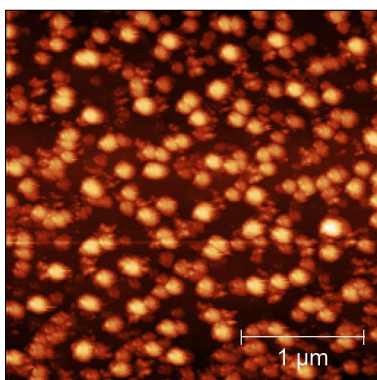
The thickness of stress relaxation layers is strongly related to the density and average size of GaN nano dots. The higher density and the smaller average size of GaN nano dots, the faster coalescence of each GaN nano dots, causing the thinner thickness of stress relaxation layer which is formed by the coalescence of GaN nano dots at pretreatment temperature. As explained above, the density and average size of GaN nano dots is affected by pretreatment temperature, HCl and NH₃ flow rate as shown in Fig 2-5. Note that the areal ratio of GaN nano dots on Al₂O₃ substrates at low pretreatment temperature is much higher than that at high pretreatment temperature. This shows a good agreement with above statement.



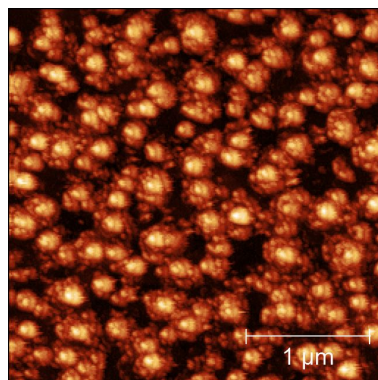
(a) 980 °C



(b) 1000 °C



(c) 1020 °C



(d) 1040 °C

Figure 2-5. Atomic force microscopy images of GaN nano dots formed on Al_2O_3 substrates at various pretreatment temperatures. The scale bar on each image is 1 μm .

Figure 2-6 is an optical microscope image showing a stress buffer layer formed between GaN nano dots on a sapphire substrate and a growing GaN layer on both of the GaN dots and the stress buffer layer. This show that the stress relaxation layer formed between the GaN dots and the GaN layer is formed when the GaN layer is grown on the sapphire substrate by using the GaN dots as buffer layers. If the thickness of stress relaxation layers is thin, the cracks in growing GaN layers were generated as depicted in Fig 2-6 (a). If the thickness of growing GaN layers is sufficient to prevent the stress evolution, a thick GaN grows without cracks. (Note that Figure 2-6 (b) shows this well.) The growing GaN layer could be grown to a thickness that is about greater than or equal to a stress relaxation layer thickness of a stress relaxation layer in which the GaN nano dots are connected to each other during the growing of the GaN layer, implying that the stress relaxation layer formed by coalescence of GaN nano dots is between the GaN dots and the GaN layer during the growing of the GaN layer. The stress relaxation layers were continuously grown at the same or substantially the same temperature as the GaN layer. When the GaN layer is grown on the GaN nano dots, dislocations may be generated at the interfaces of the GaN nano dots. The growing GaN layers were grown from each GaN nano dots and connected to

each other at a point at which the dislocations are partially removed and the stress relaxation layer is formed.

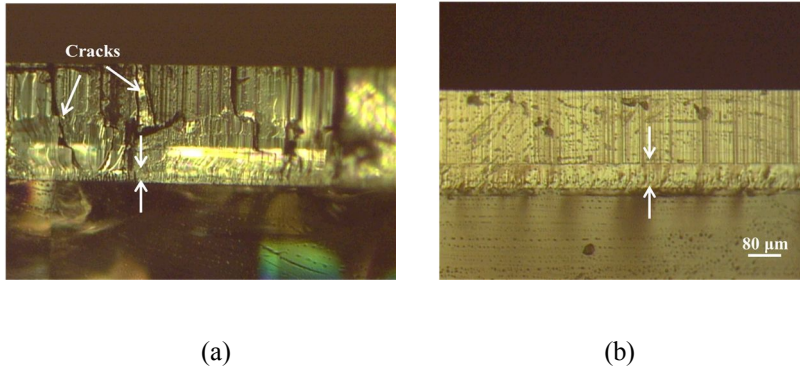


Figure 2-6. The optical microscopy image of growing GaN with buffer layers in thickness of (a) 20 μm and (b) 70 μm formed by GaN nano dots on Al₂O₃ substrates.

The density and average size of GaN nano dots defines the thickness of growing GaN layers where it has not any cracking in GaN layers. Figure 2-7 explain the dependence between the average size of GaN nano dots and critical thickness of growing GaN layers not generated for cracking in GaN layers. The stress relaxation layer have thickness of about 40 μm to about 50 μm, inclusive, as described above. The thickness of the stress relaxation layer

varies depending on the average size of the GaN dots. For example, the thickness of the stress relaxation layer may be from about 1 μm to about 100 μm , inclusive, according to the average size of the dots.

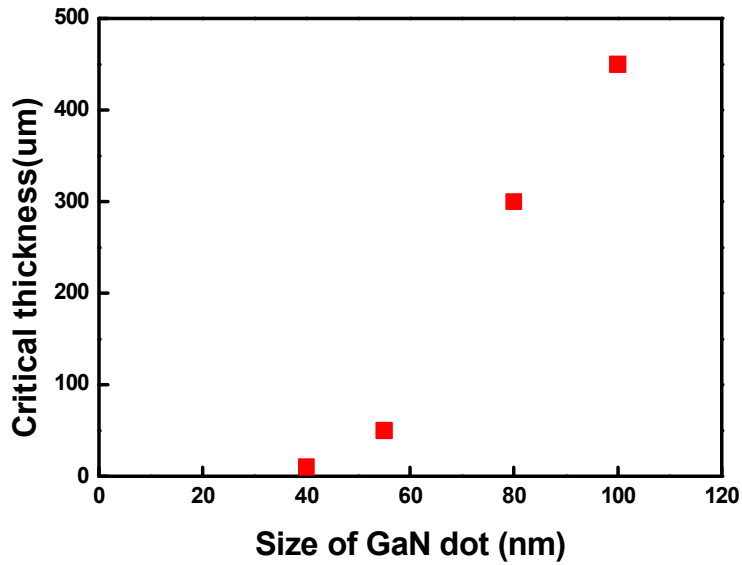


Figure 2-7. The dependence of critical thickness of growing GaN layers as a function of the average size of GaN nano dots.

When GaN is grown using GaN dots, most of which have a size of about 40 nm or greater, a stress relaxation layer thickness (coalescence), according to previous statement in which the GaN nano dots contact each other, may be about 40 μm to about 50 μm , inclusive. When the thickness of the GaN layer

is about 60 μm to about 70 μm or greater, the GaN layer have an almost mirror surface and there have few stress induced cracks, implying no stress induced cracks. When the GaN layer is grown to the stress relaxation thickness or greater, the GaN layer with few or without cracks and/or defects in the crystal may be obtained with a desired thickness range. A growing GaN layer could be grown to a thickness of about 300 μm or more (e.g., about 300 μm to about 400 μm , inclusive). When the GaN layer is grown using a relatively coarse average size of GaN dots (e.g., about 80 nm to about 100 μm , inclusive), the GaN layer have a thick thickness of about 300 μm or more. This relatively thick GaN layer can be separated from the sapphire substrate, and a freestanding GaN substrate with a sufficient thickness to be a substrate can be obtained and used for fabricating a device thereon. The GaN layer can be grown to be relatively thin (e.g., a thickness of about 300 μm or less) without creating stress induced cracks and/or defects.

Figure 2-8 presents the crystal quality of growing GaN as a function of HCl and NH_3 flow rate during pretreatment, showing that the crystal quality of growing GaN layers is strongly affected by the density and average size of GaN nano dots.

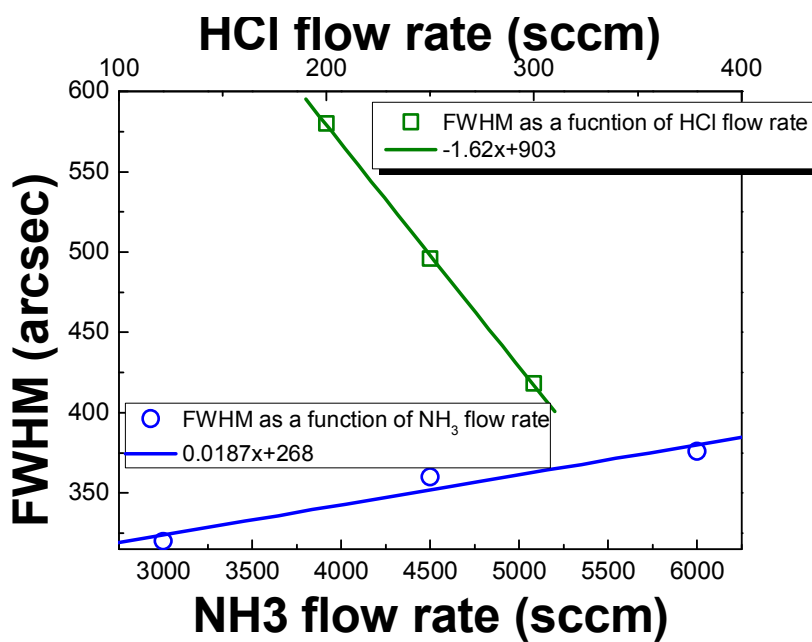


Figure 2-8. The FWHM of (0 0 0 1) X-ray rocking curve on a 300 μm -thick GaN as a function of HCl and NH_3 flow rate during pretreatment stage.

It is well known that with increasing thickness of growing GaN, the number of threading dislocations can be reduced via an interaction with themselves so that they can combine or annihilate.¹¹⁻¹³ Previously on the statement about coalescence depending on the density and average size of GaN nano dots, it commented that the agglomeration of GaN nano dots with high density and small size is much faster than that with low density and big

size, indicating 2D growth of GaN layers starts with buffer layer of thinner thickness. Therefore, the annihilation of dislocation of GaN layers with thinner buffer layer become earlier compared to that of GaN layers with thicker buffer layers.

2.3.2. Numerical analysis of gas flow rate in HVPE reactor

Considering the geometry of our HVPE system, it is difficult to obtain a thick GaN of 4 inch diameter with uniform thickness in whole wafer, surface morphology. To make it possible obtaining a 400 μm -thick GaN in 4 inch diameters, we designed HVPE with GaCl gas nozzle of tripod shape where GaCl gas could be dispersed from each gas nozzle as shown in Fig. 2-9.

Figure 2-9 demonstrates the comparison of showerhead configuration for GaCl and NH_3 gas flow between previous HVPE with one GaCl gas nozzle and HVPE of tripod shape with three GaCl gas nozzles. The surface morphology, and thickness uniformity of a thick GaN layer is governed by GaCl gas nozzle owing to the limitation of GaCl gas flow dispersion by small area of GaCl channel in one gas nozzle configuration. GaCl flow from one gas nozzle could not be dispersed uniformly into the whole area of sapphire substrates with 4 inch diameters owing to small gas nozzle area (about 1 inch

in radius). Gas nozzles of tripod shape with large GaCl gas supply area (about 2 inch in total radius), however, could provide GaCl gas flow uniformly in the whole area of sapphire substrates with 4 inch diameters.

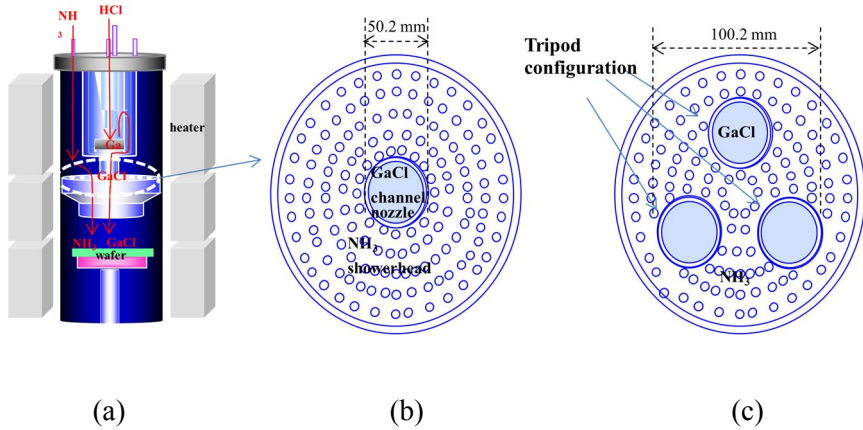
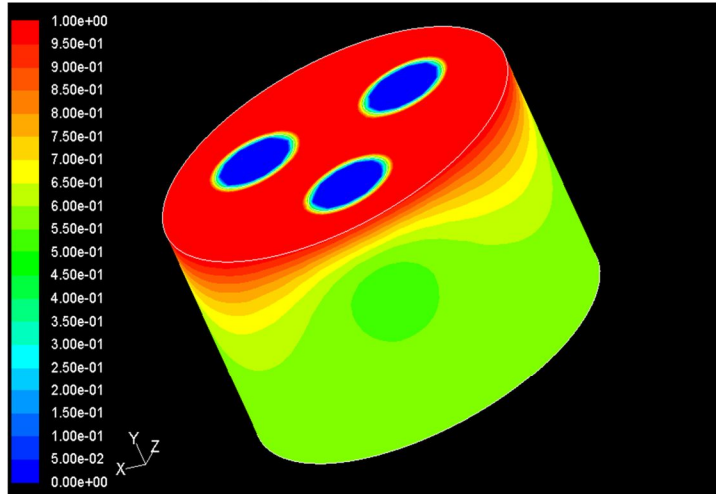


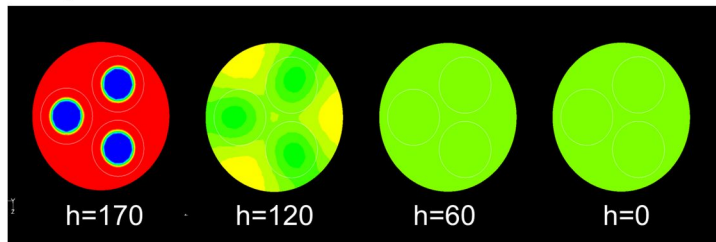
Figure 2-9. The schematics of (a) our HVPE system and its (a) one gas nozzle geometry and (b) three gas nozzles of tripod shape

To investigate the gas uniformity dependence as a function of the distance between each gas channel nozzle and wafer, we implemented FLUENT simulation for HVPE system with tripod geometry as shown in Fig. 2-10. Figure 2-10 depicts the mass fraction of GaCl and NH₃ gases as a function of distance between gas inlets and wafer.

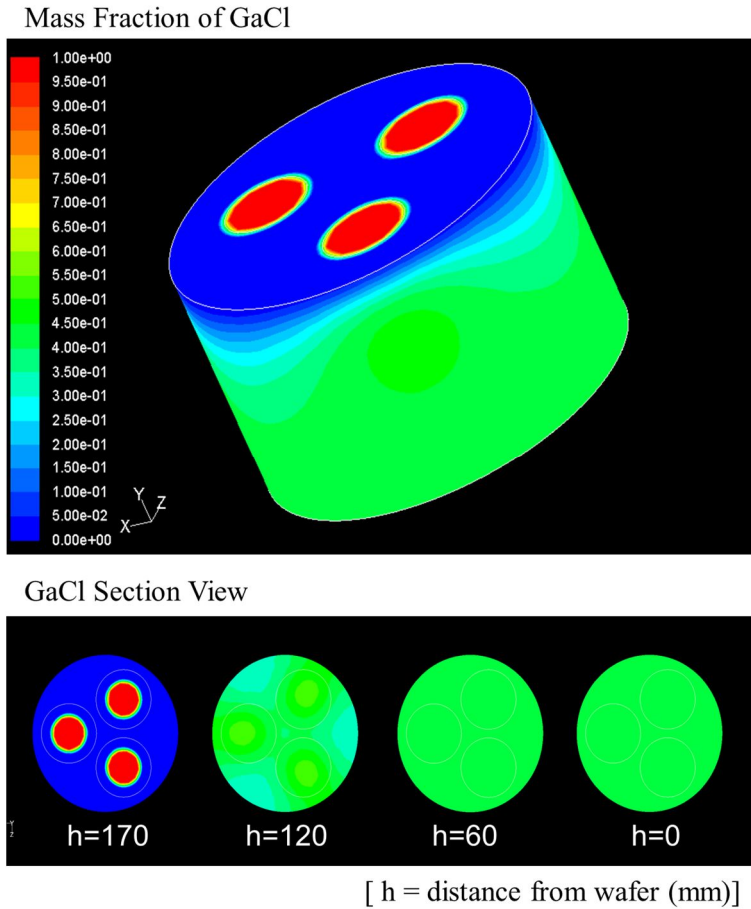
Mass Fraction of NH_3



NH_3 Section View



(a)

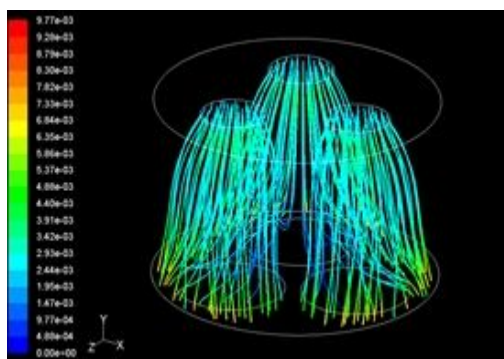


(b)

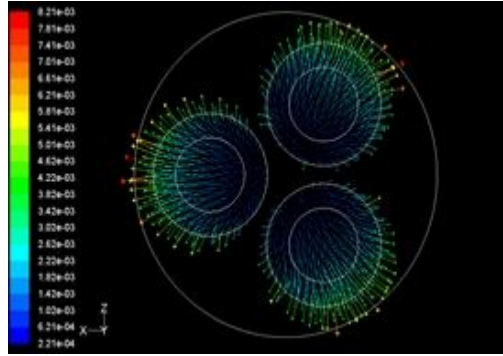
Figure 2-10. The mass fraction of (a) NH_3 and (b) GaCl gases as a function of distance between gas inlets and wafer. Gas flow rate of GaCl, NH_3 is 400 sccm, and 4800 sccm, respectively. Pressure in reactor is atmosphere, and temperature in reactor is 1000 °C

Key features of flow field for each gas are readily apparent, such as mass fraction for each gas flow at around 60 mm length from nozzle to wafer is nearly equilibrium after mixing gases at nozzle inlets.

The numerical analysis for gas flow from GaCl inlets and plane flow near susceptor is shown in Fig. 2-11, depicting the level of detailed gas flow in susceptor. Owing to stagnation of gas flow in the center of reactor, the main stream of gas is flowed to the edge of susceptor so that pressure and density of gas is high at the center of reactor. This means that the flow rate of center nozzle have to be decreased.



(a)



(b)

Figure 2-11. Numerical analysis result of (a) the gas flow from GaCl inlets and plane flow near susceptor

2.3.3. Properties of a thick GaN/sapphire and freestanding GaN

A 200 μm -thick GaN without cracks was grown on sapphire substrate with 4 inch diameters as shown in Fig. 2-12. The shape of a thick GaN layer/sapphire was convex, implying compressive stress in GaN layers originated from larger thermal expansion coefficient of sapphire than that of GaN. When released from the sapphire substrates by laser processing, the freestanding GaN substrates had a concave shape with bowing. (not shown in this chapter)

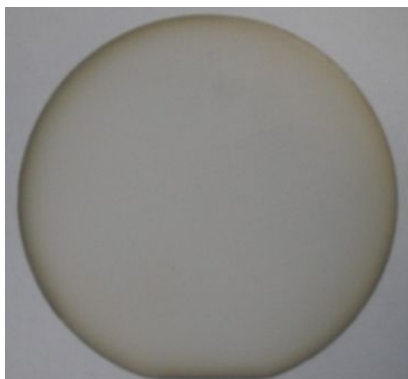
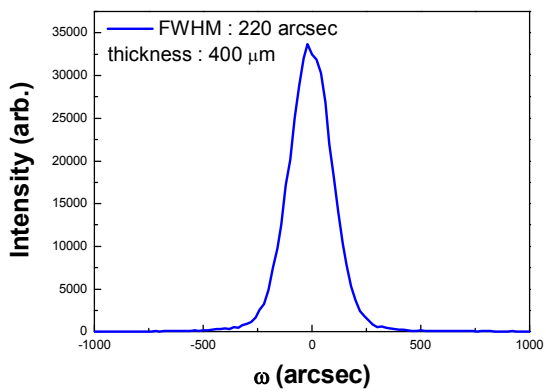
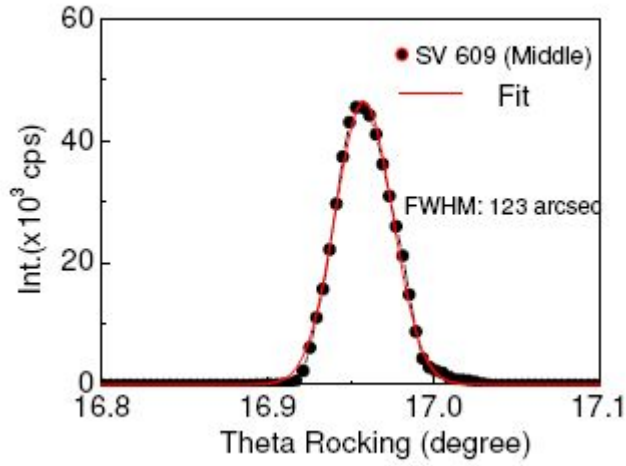


Figure 2-12. A thick GaN on sapphire substrate with 4 inch in diameters and 400 μm in thickness



(a)



(b)

Figure 2-13. X-ray rocking curve of (a) the thick GaN/sapphire (b) freestanding GaN after removing sapphire substrate

Figure 2-13 shows (0 0 0 2) X-ray diffraction ω -scan curves of 200 μm thick GaN grown on sapphire substrate. The full width at half maximum (FWHM) of the X-ray rocking curve for (0 0 0 2) diffraction of GaN/sapphire was 220 arcsec. After removing sapphire substrate, the value of FWHM of ω -scan in freestanding GaN was decreased by 123 arcsec, representing this material shows very high crystal quality.

To investigate the origin of the concave bowing of the freestanding GaN substrates, we analyzed the lattice constants of the Ga- and N-face of freestanding GaN substrates using the Bond method and compared the measured values with those for the bulk GaN crystal, i. e. strain-free GaN.¹⁴ The values of strain-free bulk GaN are $c = 5.18561$ and $a = 3.1880$ Å at room temperature, respectively. Results obtained for the Ga- and N-face of the freestanding GaN substrates are detailed in Table 2-1.

	Ga-face	N-face
Normal strain $\varepsilon_{\perp} \times 10^{-3}$ (c-axis)	-8.97	-10.42
Tangential strain $\varepsilon_{\parallel} \times 10^{-3}$ (a-axis)	2.78	7.95

Table 2-1. Residual strain of freestanding GaN

It is evident from table 2-1 that the tangential strain of the N-face of freestanding GaN substrate is larger than that of the Ga-face. Therefore, the freestanding GaN substrates have a concave shape due to the difference in residual strain for the Ga- and N-face.¹⁵ Furthermore, we confirm the crystal quality of a thick GaN/sapphire using etch pit density (EPD) measurement (thick GaN/sapphire samples were dipped in H_3PO_4 acid solution at 200 °C

during 30 min). EPD of grown sample was less than $5 \times 10^6 \text{ cm}^{-2}$ over the whole wafer surface (not shown in this chapter)

The optical characteristics of the freestanding GaN grown on sapphire substrates were obtained using PL measurements at room temperature as shown in Fig. 2-14. The strong band-edge emission peaks of the thick GaN films grown on the sapphire substrate can be observed near 3.393 eV. The FWHM of the edge peak was about 90 meV. The peak at 3.39 eV has been shown to be related to free-exiton recombination.¹⁶ The broad PL spectra was caused by the Stark effect due to the difference of the residual strain between Ga- and N-face of the freestanding GaN. The PL peaks of the samples exhibit a 78 meV red-shift with respect to those of completely relaxed bulk GaN (3.471 eV), indicating that the stress in freestanding GaN grown on the sapphire substrate is tensile in nature.^{17, 18} Otherwise, we cannot observe yellow luminescence around 2.21 eV.

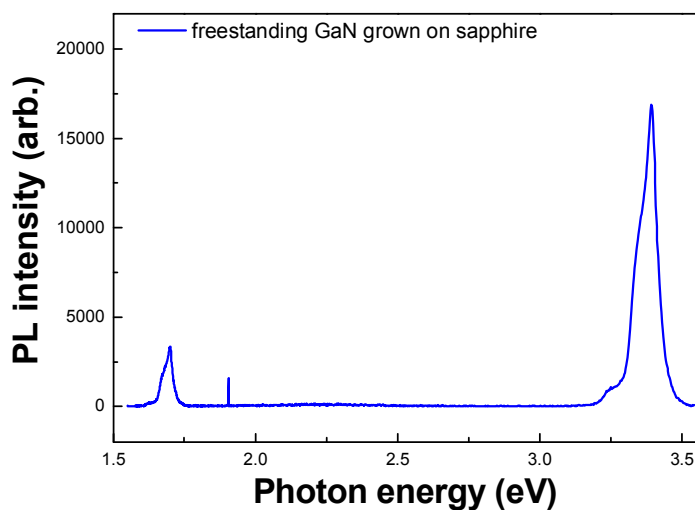


Figure 2-14. Photoluminescence spectrum of freestanding GaN grown on sapphire substrate at room temperature

2.4. Summary and conclusion

In conclusion, by forming AlN/GaN nano dots on sapphire substrate, a 400 μm thick GaN was grown on sapphire substrates with 4 inch diameters. The thickness of stress relaxation layer was determined by the density and average size of AlN/GaN nano dots. The larger size and the less density nano

dots, the slower coalescence of nano dots, making stress relaxation layer thicker. Growth parameters such as pretreatment temperature, NH_3 gas flow rate, HCl flow rate could control the density and average size of AlN/GaN nano dots. To make uniform gas flow stream in HVPE reactor, we designed new gas nozzle with tripod shape where GaCl gas flow could be delivered uniformly at proper distance (in 60 mm distance from nozzle to susceptor). Finally, a 400 μm thick GaN was grown on sapphire substrate with 4 inch in diameters. The value of FWHM in (0 0 0 2) X-ray rocking curve of a thick GaN was 220 arcsec. After lift-off of sapphire substrate, FWHM obtained for (0 0 0 2) reflection were 123 arcsec, which the bowing of wafer was changed from convex to concave, implying the tensile stress. In addition, via etch pit density measurement the crystal quality of freestanding GaN grown on sapphire substrate was confirmed. EPD density was about $5 \times 10^6/\text{cm}^2$. Photoluminescence analysis present the optical property of freestanding GaN grown on sapphire substrates. The band edge peak was on 3.393 eV which was moved to red-shift by about 78 meV compared to strain-free bulk GaN , indicating tensile stress in GaN layers.

References

- [1] Nakamura S, Senoh M, Nagahama S, Iwasa N, Yamada, T, Matsushita T, Sugimoto Y and Kiyoku H 1996 *Appl.Phys. Lett.* **69**, 4056
- [2] Ilegems M and Montgomery H 1973 *J. Phys. Chem. Solids* **34**, 885
- [3] Shintani A and Minagawa S 1974 *J. Cryst. Growth* **22**, 1
- [4] H. Larsson, D. Gogova, A. Kasic, R. Yakimova, B. Monemar, C. R. Miskys, and M. Stutzmann, 2003, *Phys. Stat. sol.(c)*. **0**, 1985
- [4] E. Valcheva, T. Paskova, S. Tungasmita, P.O.A. Persson, J. Birch, E.B. Svedberg, L. Hultman and B. Monemar, 2000, *Appl. Phys. Lett.* **76**, 1860
- [5] D. Gogova, D. Siche, A. Kwasniewski, M. Schmidbauer, R. Fornari, C. Hemmingsson, R. Yakimova and B. Monemar, 2010, *Phys. Status Solidi* **7**, 1756
- [6] A. Usui, H. Sunakawa, A. Sakai, and A.A. Yamaguchi, 1997, *Jpn. J. Appl. Phys.* **36**, L899
- [7] G. Nataf, B. Beaumont, A. Bouillé, S. Haffouz, M. Vaille, and P. Gibart, 2009, *J. Cryst. Growth.* **192**, 73

- [8] F. Lipski, T. Wunderer, S. Schwaiger and F. Scholz, 2010, *Phys. Status Solidi A* **207**, 128
- [9] W. S. Wong, T. Sands, and N. W. Cheung, 1998, *Appl. Phys. Lett.* **72**, 599
- [10] S. S. Park, I. W. Park, and S. H. Choh, 2000, *Jpn. J. Appl. Phys.* **39**, L1141
- [11] A.E. Romanov, W. Pompe, G. Beltz, and J.S. Speck, 1996, *Phys. Stat. Solidi* **198**, 3342.
- [12] X.-H. Wu, L.M. Brown, D. Kapolnek, S. Keller, B. Keller, S.P. DenBaars, and J.S. Speck, 1996, *J. Appl. Phys.* **80**, 3228.
- [13] Y. Golan, X.-H. Wu, J.S. Speck, R.P. Vaudo, and V.M. Phanse, 1998, *Appl. Phys. Lett.* **73**, 3090.
- [14] M. Leszczinski, T. Suski, H. Teisseyre, P. Perlin, I. Grzegory, J. Jun, S. Porowski, and T. D. Moustakas, 1994, *J. Appl. Phys.* **B14**, 3532
- [15] S. Park, I. Park, and S. H. Choh, 2000, *Jpn. J. Appl. Phys.* **39**, L1141
- [16] S. Chichibu, T. Azurata, T. Sota, and S. Nakamura, 1996, *J. Appl. Phys.* **79**, 2784

[17] A. Kasic *et.al.*, 2005, *J. Cryst. Growth.* **275**, e387

[18] D. Gogova, E. Talik, I. G. Ivanov, and B. Monemar, 2006, *Physica B:Condensed Matter.* **371**, 133

CHAPTER 3.

Bulk GaN with extremely low defect density by pit-assisted growth

3.1. Introduction

GaN substrates with low-dislocation density are the most promising material for the realization of power device, and high-quality violet lasers.¹⁻⁴ Among many technological approaches such as ammonothermal, high temperature high pressure (HTHP), Na flux, and MOCVD growth, hydride vapor phase epitaxy (HVPE) is regarded as the most potential and practical growth method for the commercialization of GaN substrates.⁵⁻⁷ Freestanding GaN wafers can be obtained by hetero-epitaxy technique using foreign substrates such as GaAs, SiC, and sapphire whose materials were removed after growth by special process, i. e. laser lift-off or chemical etching.⁸⁻¹² Hetero-epitaxy GaN growth, however, generates the dislocation owing to lattice mismatch between GaN and foreign substrates, which degrades the electrical and optical properties of GaN-based devices. Even if single crystal GaN substrates over dislocation density of $10^8/\text{cm}^2$ could be used for LED application, they are not available for the laser diode which requires much higher operation current density because of short lifetime. In order to realize violet laser diode and power devices, GaN single crystal substrate with large size and high quality is indispensable. (Dislocation density at least lower than $3 \times 10^6/\text{cm}^2$ is required for the application of 30 mW violet lasers¹³) Further,

higher power laser may require the single crystal GaN substrates with much lower dislocation density. Therefore, the reduction of dislocation density is a critical issue to be solved.

To overcome this issue, many researchers have been performed various approaches such as epitaxial lateral growth, patterned substrates, and dislocation elimination by epitaxial growth (DEEP).^{11,12} These methods, however, is not acceptable due to complex, high cost, and low throughput process.

In this chapter, we investigate the new pathway to obtain bulk GaN with extremely low dislocation density, namely pit-assisted growth.

3.2. Experimental details

To perform homo-epitaxial growth of GaN, freestanding GaN substrates with thickness of 400 μm were prepared. The initial etch pit density of freestanding GaN substrates was about $2.4 \times 10^6/\text{cm}^2$. To disclose the pits on the top surface of freestanding GaN as many as possible, freestanding GaN substrates were etched by HCl gas with 200 sccm at 900 °C during 5 min in HVPE reactor. Subsequently, they were dipped into H_3PO_4 acid

solution at 200 °C during 30 min to broaden pit size and increase the pit density.

The homo-epitaxial growth of GaN was carried out on prepared freestanding GaN under atmospheric pressure using N₂ as the carrier gas in downstream region of vertical hot wall type HVPE reactor where GaCl and NH₃ gas were mixed. GaCl was reacted by liquid Ga metal and HCl gas at 800 °C in the relatively upper region of the reactor.

To reduce the stress and prevent the dislocation generation during growth, the growth process are divided into 3 stages. The first is to remove the pits buried in freestanding GaN substrate. To exploit it, the initial growth temperature was heated up to 1090 °C and V/III ratio was 5, which facilitate the lateral growth of GaN nuclei, thus helping to prevent the dislocation generation. Next, it is the step for stress control, which is composed of graded stress layers. To control the stress in grown GaN layers, V/III ratio was changed from 10 to 11 where growth temperature was 1080 °C. Finally, pit removal stage is required in which V/III ratio was 8. The details of growth procedure are on Fig. 3-1. This procedure repeated by the thickness of bulk GaN with 5 mm every 1 mm thickness.

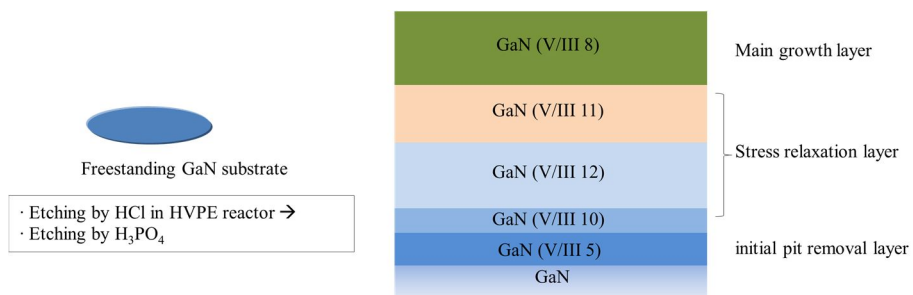


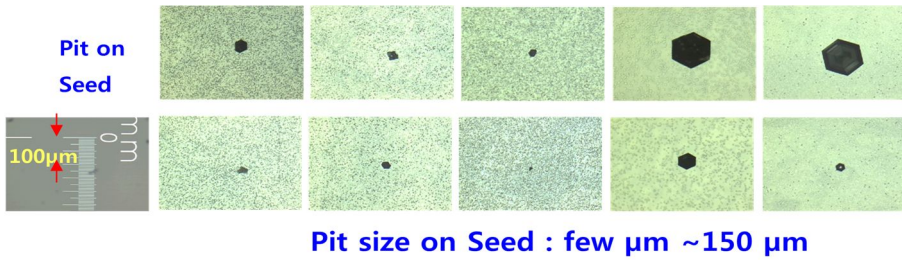
Figure 3-1. The procedure of bulk GaN growth by pit-assisted method.

The surface morphology of the grown bulk GaN layers was evaluated by atomic force microscopy (AFM) and optical microscopy. The structural properties of the grown layers were analyzed using double-crystal X-ray diffraction and transmission electron microscopy (TEM) measurements. X-ray rocking curves (ω -scan) were measured using a Cu K line ($\lambda = 0.154060$ nm) from a Bede D3 system. Plan-view TEM samples were prepared by grinding and mechanical polishing followed by ion milling. The observations were carried out at 200 kV by using a FEI F20 microscope equipped with a field emission gun. In addition, photoluminescence scanning were performed to measure the defect density of bulk GaN.

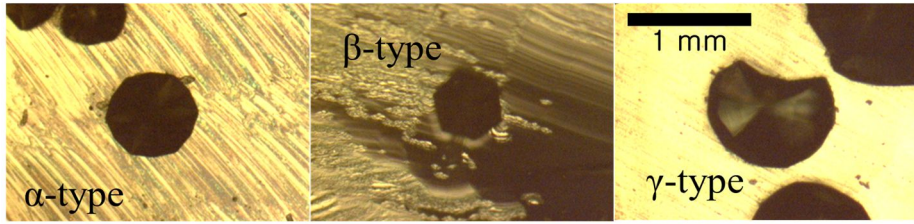
3.3. Results and Discussion

3.3.1. Pit formation revealed by HCl gas and H₃PO₄ acid solution

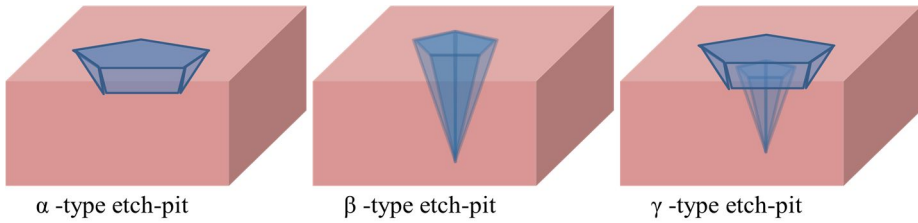
Figure 3-2 (a) illustrates the optical microscopy images of the pit generated by HCl and H₃PO₄ etching on the surface of seed freestanding GaN substrates. Most of pits are inverse-hexagonal etch pits among three kinds of etch pits, i. e. α -type etch pit is an inverse-truncated hexagonal pit, the β type one is an inverse-hexagonal pyramid, and the last γ type one is a trapezoidal type as shown in Fig. 3-2 (b) and (c). The sizes of each etch pits are varied from few μm to a few hundred μm . L. Lu *et. al.*¹⁴ revealed that the origin of etch pits are related to the dislocation type, in which α -, β -, γ - type etch pit correspond with screw, edge, and mixed dislocation, respectively.



(a)



(b)



(c)

Figure 3-2. The optical microscopy images of (a) pits with various size revealed by HCl and H₃PO₄ etch on freestanding GaN, (b) three types of pits, and (c) the schematics of profiles for three kinds of etch pits.

It is well known that a screw dislocation creates a step when it terminates at the GaN surface. This step is associated with the natural terrace structure. Etching enlarges the step, thus forming a few spiral steps. So easily attacked is a spiral step, finally leaving the small plane with Ga-face surface. Once Ga-face surface is revealed, the lateral etching rate will be dominant to make shape of pits, implying enlargement of small planes. Therefore, the shape of screw dislocation can be inverse-truncated hexagonal shape.

Meanwhile, inverse hexagonal pyramid shape corresponds to edge dislocation, which is vertical to the surface, indicating the dangling bond is on the vertical direction. The etch rate of dangling bond is so high that there will be few chance to stop the etch in vertical direction, thus resulting the inverse- hexagonal pyramid shape. Finally, γ -type etch pit is related to the mixed dislocation. Since the characteristics of mixed dislocation has components of both screw and edge dislocation, it is clear that the shape of γ -type etch pit is synthesized by those.¹⁴

X. H. Wu *et.al.*¹⁵ has it that edge dislocations represent a significant fraction of the total dislocation density in GaN layers, especially much more in thicker films. They studied thick GaN films over 5 μm and revealed that the edge threading dislocations make up 40% of the total threading dislocation density in 1 μm thick GaN layers, while after growing over 5 μm , they take up over 70% of all threading dislocations. On the other hand, pure screw dislocations are rare type of threading dislocations. Published TEM analysis usually counts screw dislocations at 1 to 10% of the overall threading dislocation density in MOCVD-grown material.¹⁶ Wu *et al.* reported that pure screw threading dislocations had much less than 1% of the total threading dislocation density in MOCVD-grown GaN.¹⁵ However, depending on the growth method, screw dislocations have been found to represent 20% of the overall TD density for MBE-initiated GaN.¹⁶ Nanopipes,

which are sometimes observed in GaN films grown on SiC and on sapphire, have been associated with open-core screw dislocations.¹⁷ Nanopipes are surrounded by growth spirals at the film surface, indicating a c-component Burgers vector dislocation at their centers.¹⁷ However, nanopipes appear not to have appreciable density in high-quality material, and often screw dislocations have closed cores.¹⁶ It is not presently understood why open core dislocations occur, or why screw dislocations have low density in epitaxial GaN films.¹⁸ This might be related to the dislocation inclination of screw dislocations. This, however, need to be explicit.

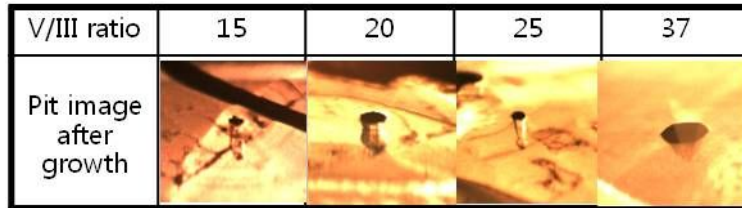
Likewise, freestanding GaN as a seed substrate shows similar results for proportion of dislocation type, indicating edge dislocation counting over 85%, screw dislocations on below 10%, and mixed dislocation with about 5%.

3.3.2. Pit annihilation during growth

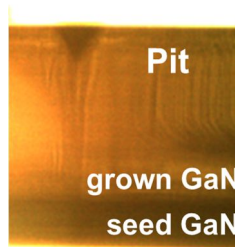
As noted in previous section 3.2, bulk GaN was grown on varying V/III ratio to control the pit behavior and stress evolution. It takes granted for that the growth parameters can affect the properties of growing GaN such as stress, crystal quality, and defect density. In particular, defect density can be prevented by lowering V/III ratio, which promotes the lateral growth rate of

GaN nuclei, resulting in the dislocation annihilation in earlier growth. In addition, we expect the same phenomena by increasing growth temperature. This is why the initial growth was performed in growth temperature of 1090 °C and V/III ratio with 5, respectively.

Figure 3-3 shows the optical microscopy image of pit shape as a function of V/III ratio after growing GaN in thickness of 800 μm.



(a)



(b)

Figure 3-3. The optical microscopy image of (a) pit shape as a function of V/III ratio after growing 1.2 mm-thick GaN on freestanding GaN with 400 μm (b) cross sectional microscopy image of bulk GaN with 1.2 mm thickness.

The interface between growing GaN and seed GaN is easily shown by contrast difference.

All pits are started from the interface between growing GaN and seed GaN. With increasing V/III ratio, the size of pits expands. With decreasing V/III ratio, the opposite results come. The pit shapes are varied as follows; annihilation, intact, and expansion ones as shown in Fig 3-4.

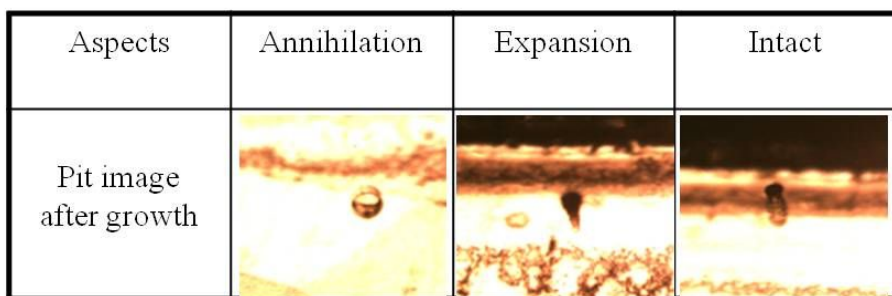


Figure 3-4. The optical microscopy image of pit shape.

In annihilation behavior, the pits are removed during GaN growth, which is attributed to the promoted lateral growth rate of GaN nuclei. In intact, pits are growing without any expansion or annihilation, which is likely to originate from the balance of GaN nuclei migration rate along c-axis and in-plane. In expansion, pits are expanded and the pit size can be few micron to few millimeters. As an example, the pit size on the surface of bulk GaN

with 3.0 mm thickness can be increased by 2 mm diameters where V/III ratio is 37 as shown in Fig. 3-5.


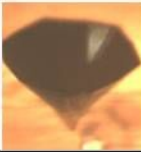
V/III ratio	37 (1.2 mm)	37 (3 mm)
Pit image After growth		

Figure 3-5. The optical microscopy image of expanded pits on V/III ratio with 37 as a function of growing GaN thickness.

3.3.3. Mechanism of dislocation annihilation¹⁹

K. Motoki *et.al.*¹⁹ reported that dislocations are concentrated into the bottom of the hexagonal pits and dislocations are rare in other areas. Via cross sectional TEM analysis, they revealed that a bundle of dislocations about 100 nm wide are seen at the center of hexagonal pit. Furthermore, they showed that many dislocations are aligned to $\langle 1\bar{1}00 \rangle$. It suggests that even at the edge lines dislocations would propagate to the center of the pit along $\langle 1\bar{1}00 \rangle$ as the $\{11\bar{2}2\}$ facets grow like the manner of ELO. According to above results, they suggested a new model to explain dislocation reduction mechanism. The model is explained as shown in Fig. 3-6, when a hexagonal

pyramidal pit with $\{11\bar{2}2\}$ facets is generated and goes on, dislocations existing on the surface of facets begin to on its way, i. e. parallel to (0001) plane mainly to the direction of $\langle 11\bar{2}0 \rangle$ and concentrate toward the center of the hexagonal pit. It is considered that from various routes on 6-fold symmetry are possible for propagation of dislocation on a-position as shown in Fig. 3-6(c). A dislocation on a position in Fig. 6(c) running parallel to $\langle 11\bar{2}0 \rangle$ will meet the boundary of adjacent $\{11\bar{2}2\}$ facets and then merge into the $\langle 1\bar{1}00 \rangle$ direction along the boundary together with other dislocations. When dislocations reach the center, then they begin to run upward along the c-axis in a group as the growth proceeds. Through this phenomena, dislocations always are concentrated at the center, and therefore dislocations can get cleaned within the hexagonal pyramidal pits except for its center.¹⁹

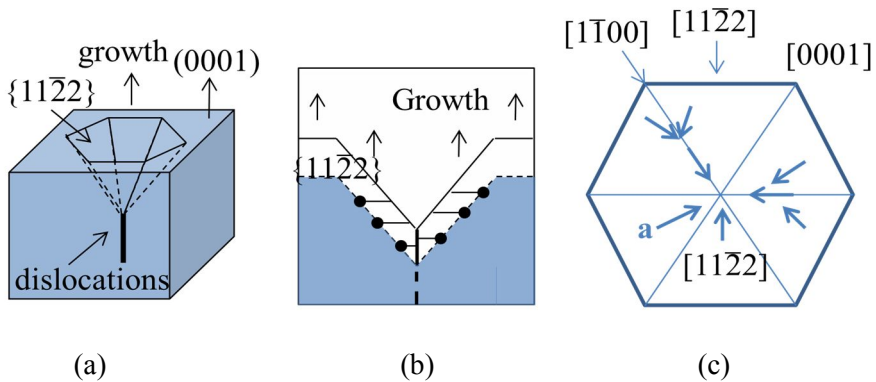


Figure 3-6. Schematic diagram of dislocation reduction mechanism: (a) diagram of growth with hexagonal pits constructed by $\{11\bar{2}2\}$ facets concentrating dislocations at the bottom of the pit; (b) diagram of the dislocation propagation from the surface of the facets to the center of the pit; (c) plan-view of the dislocation propagation route within the hexagonal pit.

If we can form hexagonal pits to apply for this effect intentionally, the threading dislocations can be cleaned, and the propagation of them can be restricted during growth. Therefore, we employed that the other area other than hexagonal pits is treated in the growth of GaN, and by sweeping V/III ratio, and growth temperature to enhance the block of pit, propagation and generation of hexagonal pits during the growth from the early stage to the end of the growth are restricted. Thus, dislocations could not propagate along growth direction, and finally underwent the annihilation. Referring to this mechanism, we tried to form etch pit as many as possible, and then employed the removal of pits and the prevention of pit generation.

3.3.4. Suppression of polycrystalline GaN generation

Polycrystalline GaN can be commonly observed during homoepitaxial

GaN growth, which is related to the behavior of GaN nuclei during growth stage.

Figure 3-7 demonstrates that the optical microscopy image of bulk GaN with 2 mm thickness in cross sectional view.

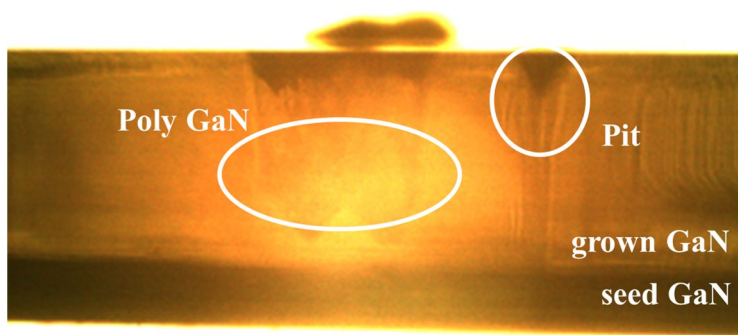


Figure 3-7. Cross-sectional optical microscopy image of bulk GaN with 2 mm thickness.

Polycrystalline GaN and pits were generated from the seed GaN substrates as depicted in Fig. 3-7. Therefore, it is essential to improve the crystal quality of grown GaN during growth stage.

To employ it, we tried two kinds of approaches: the supplement of additional HCl flow and decrease in V/III ratio. Once the polycrystalline GaN

nuclei were created, it can propagate through bulk GaN. Additional HCl gas can play role to eradicate by etching created polycrystalline GaN nuclei without significant etch of single crystalline GaN owing to bonding energy difference between single crystalline GaN and polycrystalline one. Thus by increasing additional HCl flow rate, we can decrease or prevent the polycrystalline GaN propagation via bulk GaN growth as shown in Fig. 3-8.




Additional HCl flow rate (sccm)	0	40	100
Result			
Remark	- Poly GaN		- No Poly GaN - Many pits

Figure 3-8. Additional HCl flow rate vs polycrystalline GaN in bulk GaN.

Furthermore, polycrystalline GaN generation can be prevented by decreasing V/III ratio during growth as shown in Fig. 3-9, implying too much growth rate causes negative effects on homoepitaxial growth. This may come from the fast nucleation of GaN before the migration of GaN nuclei into

stable site on GaN substrate. Too low V/III ratio can result in the increment of stress in grown GaN layer so that appropriate V/III ratio will be optimized.



V/III ratio in main growth	30	38
Result		

Figure 3-9. V/III ratio vs polycrystalline GaN in bulk GaN.

3.3.5. Suppression of micro cracks in bulk GaN

Owing to low V/III ratio to prevent pit generation in main growth stage, the stress can be evolved in growing GaN layer, which leads to the micro cracks existing commonly near the surface of bulk GaN. Even if there is no difference of physical properties such as lattice constant and thermal expansion coefficient in homo-epitaxial growth, it is noticeable that the crystal quality difference between growing GaN and grown GaN exists,

resulting in stress evolution. By varying V/III ratio during stress relaxation layer and main growth, the micro cracks creation could be neglected. Figure 3-10 explains V/III ratio variation during growth and micro cracks evolution in bulk GaN.

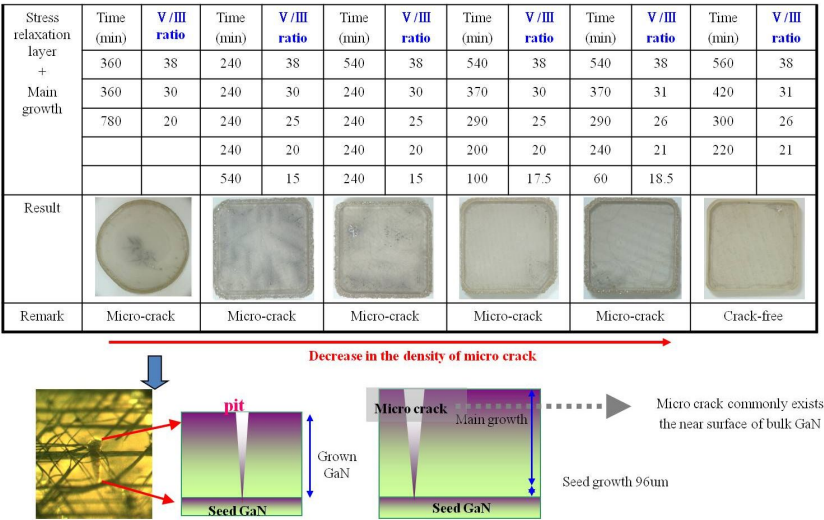


Figure 3-10. Experiment condition of bulk GaN and schematics for micro crack.

3.3.6. Properties of bulk GaN with 5 mm in thickness

Figure 3-11 shows a photograph of GaN single crystal with 3" in size and 5 mm in thickness, which was realized by pit-assisted growth method to

form extremely low defect density. No cracks were observable. The bulk GaN has a mirror-like surface and is transparent.

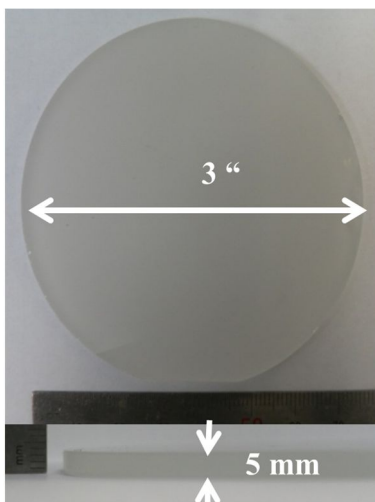
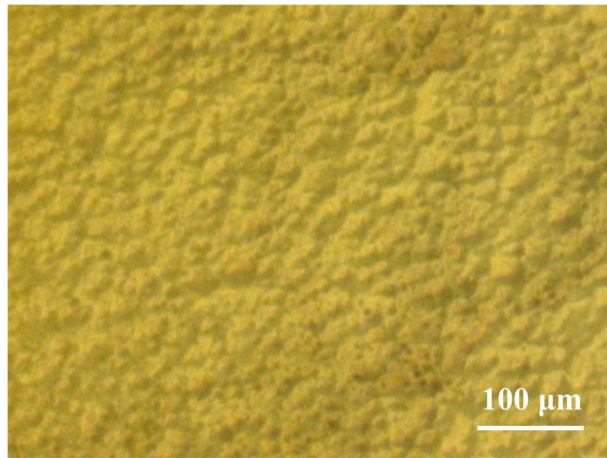


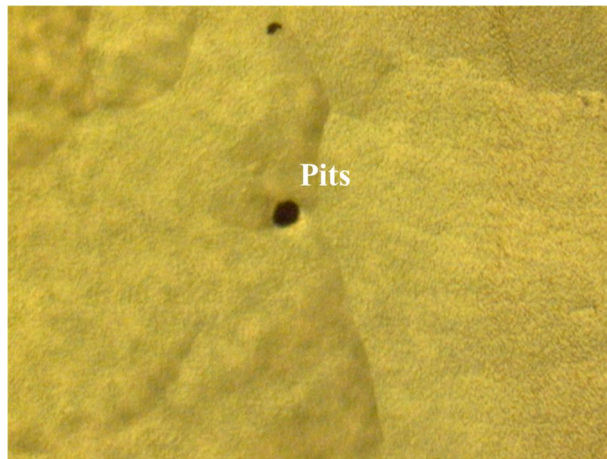
Figure 3-11. A photograph of bulk GaN with 5 mm thickness and 3 inch diameters grown by pit-assisted growth.

Even if the thickness of bulk GaN is very thick, hillocks on the surface of bulk GaN with 5 mm thickness is not readily observable. In some area, hillocks with hexagonal sides can be observed as explained in Fig 3-12. We expect that relative planar surface of bulk GaN comes from the low V/III ratio in main growth stage. Indeed, hexagonal hillocks can occasionally represent in large sizes, to the extent that they are individually visible to the

naked-eyes. When viewed with an optical microscope, spiral growth steps are usually visible as illustrated in Fig. 3-12(b). Promoted diffusion of GaCl, however, restricts the development of hillocks on the bulk GaN owing to low V/III ratio.



(a)



(b)

Figure 3-12. The optical microscopy images on the surface of bulk GaN.

The crystal quality of bulk GaN with 5 mm in thickness was evaluated by X-ray rocking curve for (0 0 0 2) diffraction where the value of the full-width at half maximum (FWHM) was 28 arcsec as depicted in Fig. 3-13. Indeed, the resolution limit of X-ray diffractometer (≥ 30 arcsec) cannot make it possible to evaluate the real crystal quality of bulk GaN. To make it clear, etch pit density (EPD) measurement was employed in which bulk GaN was dipped into H_3PO_4 acid solution at 200 °C during 30 min. It revealed that the distribution of etch pit is not homogeneous but random, and the EPD was counted as low as $3 \times 10^2/\text{cm}^2$. This value is the best result in GaN as long as we've investigated.

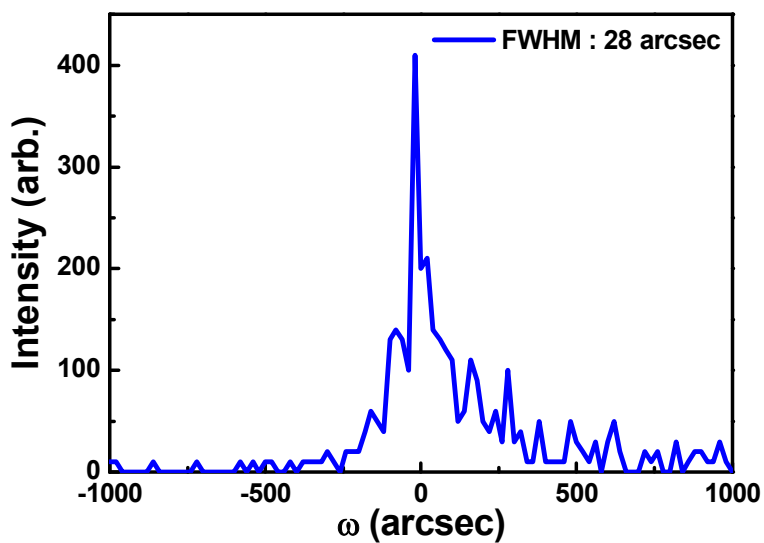


Figure 3-13. (0 0 02) X-ray rocking curve of bulk GaN with 5 mm in thickness.

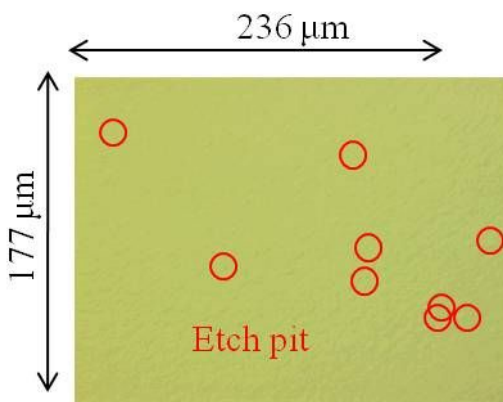
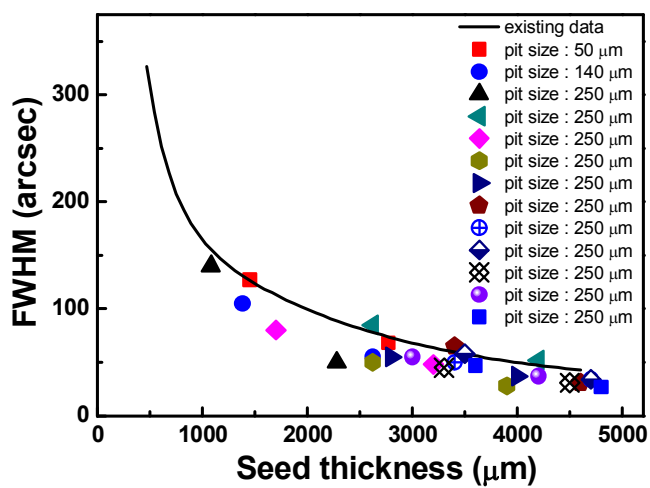


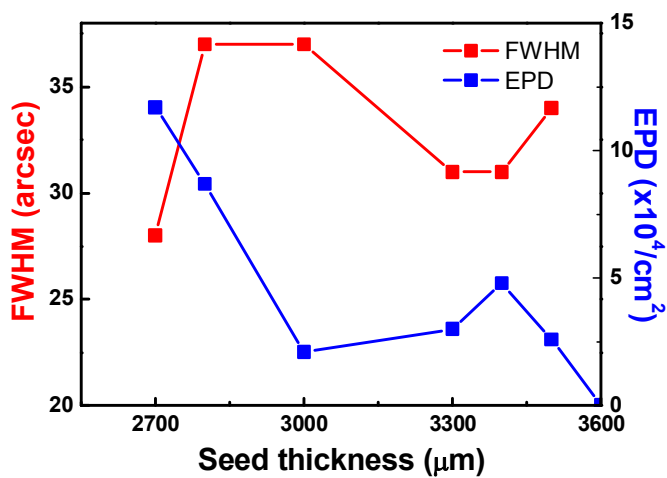
Figure 3-14. The optical microscopy image of bulk GaN after dipping

in H_3PO_4 acid solution at 200 °C during 30 min.

Figure 3-15 represent the crystal quality of bulk GaN as a function of thickness. The crystal quality of bulk GaN depending on the size of pits formed in freestanding GaN substrates is shown in Fig. 3-15(a). It is noticeable that there is no correlation between the size of pits and crystal quality of bulk GaN . Once pits are occurred, dislocations are concentrated at the center of them. Even though the size of pits are expanded, the degree of dislocation gathering into the center of pits will not be related to the size of pits, but the density of pits, we consider. As the film thickness increases, the possibility of the dislocations reaction increases. This phenomena is well known in GaN growth. Dislocations may react with one another when they are close enough. Two threading dislocation lines may become one threading dislocation with the new Burgers vector $b_3 = b_1 + b_2$, and this reaction is called fusion. If these two threading dislocation lines have the opposite Burgers vectors ($b_1 = -b_2$), then the reaction becomes annihilation; these two threading dislocation lines are removed entirely because $b_1 + b_2 = 0$. Fusion and annihilation reactions are the primary mechanisms for the density reduction of threading dislocations.²⁰



(a)



(b)

Figure 3-15. (a) bulk GaN thickness with varying pit size vs FWHM of (0 0 0 2) X-ray rocking curve, and (b) bulk GaN thickness vs FWHM and EPD.

3.4. Summary and Conclusions

In conclusion, pit-assisted growth method of GaN was employed by intentional formation of etch pit on the Ga-face of freestanding GaN. To perform it, freestanding GaN substrate was handled by HCl gas treatment at 900 °C in HVPE reactor, and subsequently dipped into H₃PO₄ acid solution at 200 °C during 30 min. The etch pits generated by intentional pit formation, is composed of three kinds of types: α -type etch pit - an inverse-truncated hexagonal pit, the β type one - an inverse-hexagonal pyramid, and the last γ type one - a trapezoidal type. Each etch pit types are related to the screw, edge, and mixed dislocation, respectively. Similarly to the results from other freestanding GaN, most of etch pits consists of β type etch pit, originating from the edge dislocations. This means that screw dislocations are readily annihilated by increasing the thickness of GaN.

By applying pit-assisted growth method, bulk GaN with 5 mm in thickness, and 3 inch in size, respectively was grown. The surface of bulk GaN is relatively plain, and transparent. FWHM of X-ray rocking curve at (0 0 2) diffraction was 28 arcsec, and the value of EPD was evaluated by $3 \times 10^2/\text{cm}^2$, indicating very extremely high crystal quality. This is achieved by the annihilation of pits during growth. Because dislocations propagate into the center of pits, the crystal quality of bulk GaN could be improved by preventing pit generation and removing pits. The application of bulk GaN with extremely low defect density is not clear, yet. Notwithstanding, we expect that the realization of such a extremely high crystal quality bulk GaN makes it possible to improve the device performance requiring the high crystal quality of substrate and growing layers such as power device and laser diodes.

References

- [1] H. Amano, N. Sawaki, I. Akasaki and Y. Toyoda, 1986, *Appl. Phys. Lett.* **48**, 353
- [2] S. Nakamura, 1991, *Jpn. J. Appl. Phys.* **30**, L1705
- [3] S. Nakamura, M. Senoh, N. Iwasa, S. Nagahama, T. Yamada and T. Mukai, 1995, *Jpn. J. Appl. Phys.* **34**, L1332
- [4] S. Nakamura, M. Senoh, S. Nagahama, N. Iwasa, T. Yamada, T. Matsushita, H. Kiyoku, Y. Sugimoto, T. Kozaki, H. Umemoto, M. Sano and K. Chocho, 1998, *Appl. Phys. Lett.* **72**, 211
- [5] S. Porowski, and I. Grzegory, 1997, *J. Crystal Growth*, **178**, 174
- [6] T. Hashimoto, K. Fujito, M. Saito, J.S. Speck, and S. Nakamura, 2005, *Jpn. J. Appl. Phys.* **44**, L1570
- [7] F. Kawamura, H. Umeda, M. Morishita, M. Kawahara, M. Yoshimura, Y. Mori, T. Sasaki, and Y. Kitaoka, 2006, *Jpn. J. Appl. Phys.* **45**, L1136
- [8] M.K. Kelly, R.P. Vaudo, V.M. Phanse, L. Gorgense, O. Ambacher, and M.

Stutzmann, 1999, *Jpn. J. Appl. Phys.* **38**, L217

[9] S.S. Park, I.W. Park, and S.H. Choh, 2000, *Jpn. J. Appl. Phys.* **39**, L1141

[10] Y. Kumagai, H. Murakami, A. Koukitu, K. Takemoto, and H. Seki, 2000, *Jpn. J. Appl. Phys.* **39**, L703

[11] K. Motoki, T. Okahisa, N. Matsumoto, M. Matsushima, H. Kimura, H. Kasai, K. Takemoto, K. Uematsu, T. Hirano, M. Nakayama, S. Nakahata, M. Ueno, D. Hara, Y. Kumagai, A. Koukitu, H. Seki, 2001, *Jpn. J. Appl. Phys.* **40**, L140

[12] K. Motoki, T. Okahisa, S. Nakahata, N. Matsumoto, H. Kimura, H. Kasai, K. Takemoto, K. Uematsu, M. Ueno, Y. Kumagai, A. Koukitu, and H. Seki, 2002, *J. Crystal Growth.* **237**, 912

[13] O. Matsumoto, S. Goto, T. Sasaki, Y. Yabuki, T. Tojyo, S. Tomiya, K. Naganuma, T. Asatsuma, K. Tamamura, S. Uchida, M. Ikeda, in: Extended Abstracts of the 2002 International Conference on Solid State Devices and Materials, Nagoya, 2002, p. 832.

[14] L. Lu, Z. Y. Gao, B. Shen, F. J. Xu, S. Huang, Z. L. Miao, Y. Hao, Z. J.

Yang, 2008, *J. Appl. Phys.* **104**, 123525

[15] N. Grandjean, J. Massies, P. Venn!egu"es, M. Leroux, F. Demangeot, M. Renucci, J. Frandon, 1998, *Appl. Phys.Lett.* **83**, 1379

[16] Y. Xin, S.J. Pennycook, N.D. Browning, P.D. Nellist, S. Sivananthan, F. Omn"es, B. Beaumont, J.P. Faurie, P. Gibart, 1998, *Appl. Phys.Lett.* **72**, 2680

[17] W. Qian, G.S. Rohrer, M. Skowronski, K. Doverspike, L.B. Rowland, D.K. Gaskill, 1995, *Appl. Phys.Lett.* **67**, 2284

[18] S. K. Mathis, A. E. Romanov, L. F. Chen, G. E. Boltz, W. Pompe, J.S. Speck, 2001, *J. Crystal Growth.* **231**, 371

[19] K. Motoki, T. Okahisa, S. Nakahata, K. Uematsu, H. Kasai, N. Matsumoto, Y. Kumagai, A. Koukitu, and H. Seki, Proc. 21st Century COE Joint Workshop on Bulk Nitrides IPAP Conf. Series 4, 32

[20] J. Li, 2007, *Mechanism of threading dislocation reduction in GaN by in-situ SiH₄ treatment* (Doctoral dissertation). Retrieved from ProQuest Dissertations and Theses. (Accession Order No. 3272464)

CHAPTER 4.

The fabrication of freestanding GaN on Si substrate via in-situ removal of Si substrate

4.1. Introduction

GaN has gained considerable attention as a material suitable for use in optoelectronic and electronic devices because of its excellent physical properties such as its wide band gap, high thermal conductivity, and high breakdown voltage.¹⁾ Because of the lack of commercially available GaN substrates with large diameters, present commercial GaN-based devices must be fabricated by epitaxy onto foreign substrates such as sapphire, SiC, and GaAs. The heteroepitaxial growth of GaN, however, results in high dislocation densities ($10^7 \sim 10^{10} / \text{cm}^2$), which deteriorates its optical and electrical properties.²⁾ As an alternative, the use of freestanding GaN wafers could possibly circumvent the above-mentioned problems. Even though HVPE is currently used as a practical method for preparing freestanding GaN wafers due to its high growth rate and crystal quality, up to now there are still obstacles such as size limitations (≤ 6 inches in diameter) and high production costs that restrict the commercial success of freestanding GaN wafers.³⁾

The use of Si wafers as substrates to fabricate GaN wafers can be a feasible solution to such problems. However, it has been impossible to grow a thick GaN layer on a Si substrate using conventional methods because of the large lattice mismatch (16.9%) and the difference between the thermal

expansion coefficients of GaN ($\alpha_a = 5.59 \times 10^{-6}/\text{K}$) and Si ($\alpha_a = 3.77 \times 10^{-6}/\text{K}$). These factors result in cracks when the reactor cools down from the growth temperature to room temperature after the growth of GaN, and high bowing.⁴⁾ Moreover, the meltback effect - the reaction of Ga and Si due to the out-diffusion of Si atoms into GaN layers - makes it even more difficult to grow GaN on a Si substrate.⁵⁾

Yang *et al.*⁶⁾ employed the GaN layer with 1 μm in thickness on Si substrate using funnel-like GaN nano rod buffer layer and Ishikawa *et al.*⁷⁾ demonstrated the growth of a 1 μm thick GaN layer on a Si substrate using an intermediate buffer layer consisting of AlN and AlGaIn. The intermediate buffer layer essentially serves to reduce the meltback effect during growth. However, these are not effective enough to overcome the issues related to the growth of thick GaN layers on Si substrates.

In this chapter, 2 inch freestanding GaN wafer was grown from Si wafer using in situ removal of the substrate in HVPE. This will be able to provide a way to the fabrication on large-sized freestanding GaN (over 8 inches in diameter) on Si substrates in the near-future.

4.2. Experimental details

Schematic illustration of the steps involved in the fabrication of a freestanding GaN on a Si substrate is detailed in Fig. 4-1. A 2 inch (111) Si wafer was used as a substrate for the growth of the GaN layer. Prior to the growth, the Si substrate was cleaned using $\text{H}_2\text{SO}_4:\text{H}_2\text{O}_2:\text{H}_2\text{O}$ (3:1:1) and HF (6%) solutions to obtain a hydrogen-terminated surface and an oxygen-free Si substrate, respectively. Furthermore, to prevent the meltback and release the stress due to the lattice mismatch between the Si substrate and GaN layer, a 100 nm thick AlN buffer layer was deposited on the Si substrate using metalorganic chemical vapor deposition (MOCVD). For this process, trimethylaluminium (TMAI) and NH_3 were used as source materials and hydrogen was employed as a carrier gas for deposition at a pressure of 100 Torr at 1000 °C. After AlN deposition, a 500 nm thin GaN layer with the value of 250 arcsec and 350 arcsec in (0002) and (10-12) X-ray rocking curve, respectively, was grown at the same temperature using MOCVD. Subsequently, a 400 μm thick GaN layer was grown on the GaN/AlN/Si substrate using a hydride vapor phase epitaxy (HVPE) system with capability of etching the substrate. For the HVPE growth, HCl was pre-reacted with liquid Ga to form GaCl gas, which was transported to the growth zone at

1000 °C. At the growth zone, the GaCl gas reacted directly with NH₃, resulting in the deposition of the GaN layer on the Si substrate with MOCVD GaN/AlN layers. Here, N₂ was used as a carrier gas, and the V/III ratio was 20. Subsequently, the Si substrate was etched by HCl gas at about 1000 °C before the HVPE reactor was cooled down to room temperature. Finally, a freestanding GaN was obtained.

The structural properties of the freestanding GaN were analyzed using double crystal X-ray diffraction and etch pit density (EPD) measurements. X-ray rocking curves (ω -scan) were measured using Cu K line ($\lambda=0.154060$ nm) from Bede D3 system. To measure etch pit density, freestanding GaN was etched in H₃PO₄ for 20 minutes at 200°C and then observed in optical microscope. In addition, the optical properties were determined by photoluminescence (PL) measurements at 10 K using excitation by a He-Cd laser of wavelength 325 nm.

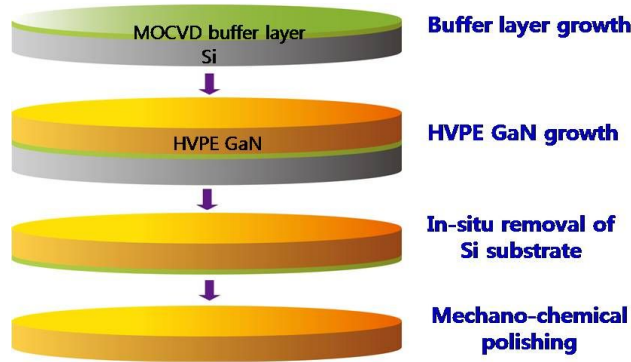


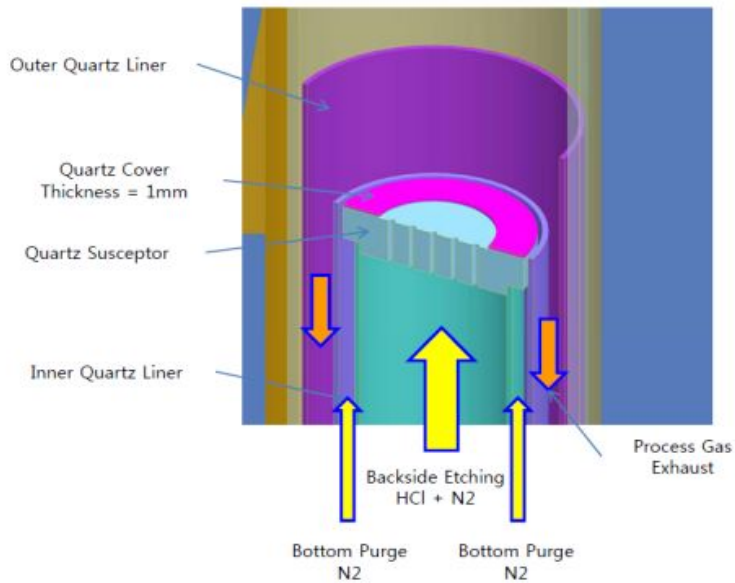
Figure 4-1. Schematic illustration of the steps for fabrication of a freestanding GaN on a Si substrate using in-situ Si etching.

4.3. Results and Discussion

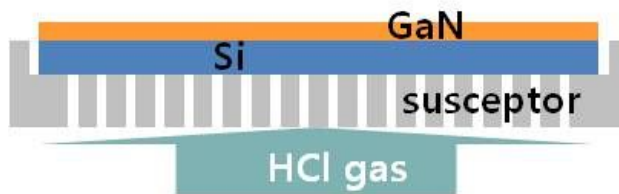
4.3.1. Design of HVPE reactor for in situ removal of Si substrate

To realize a new concept growth of freestanding GaN, HVPE reactor was modified into the configuration with special gas nozzle and susceptor to remove Si substrates at high temperature as shown in Fig. 4-2.

Figure 4-2 illustrates the schematics of HVPE reactor for in-situ removal of Si substrate, which was achieved by special gas nozzle and susceptor structure where HCl gas can flow through susceptor from bottom side of the support in HVPE reactor.



(a)



(b)

Figure 4-2. Schematic diagram of (a) HVPE reactor designed to remove Si substrate at high temperature, and (b) susceptor design to remove Si substrate. Si substrates can be removed by HCl gas flowed from backside in susceptor.

To etch Si substrate at high temperature, additional HCl gas nozzle was added to the bottom of support to hold the quartz susceptor where channels to flow HCl gas were carved.

4.3.2. Numerical analysis for in situ removal of Si substrate

When a Si wafer is used as a substrate for the growth of GaN, the main hindering factor is the tensile stress that originates from a combination of the difference between the thermal expansion coefficients and the lattice mismatch. Under such conditions, the residual stress in the GaN layer can be expressed as⁸⁾

$$\sigma_T = \sigma_{EL} + \sigma_{TH} \quad (1)$$

where σ_T is the residual stress, σ_{TH} is the thermal stress due to the difference in thermal expansion coefficients between the GaN layer and the Si substrate, and σ_{EL} is the elastic stress due to the lattice mismatch between the GaN layer and Si substrate at the typical growth temperature.

σ_{TH} and σ_{EL} can be described by following equations :

$$\sigma_{EL} = \frac{E \varepsilon_{misf}(h)}{1 - \nu} \quad (2)$$

$$\sigma_{TH} = \frac{(\alpha_s - \alpha_f)(T - T_g)E_f}{1 - \nu_f} \quad (3)$$

where E stands for the Young's modulus, and $\varepsilon_{misf}(h)$ the strain by misfit at the certain thickness. ν and ν_f is the Poisson's ratio of substrate and film. α_s , and α_f are the thermal expansion coefficient of substrate and film, respectively. T is room temperature, and T_g growth temperature.

The thermal stress σ_{TH} is the main issue for the growth of thick GaN layer on Si substrates. It is possible to make the value of σ_{TH} negligible if the Si substrate is removed in-situ at a high temperature, right after the growth of GaN, before it is cooled down to room temperature. This would essentially nullify the stress evolution in the GaN layer. On the basis of the aforementioned theory, we concluded that the instant removal of Si substrate can prevent the tensile stress accumulation during cooling down after the growth of HVPE GaN layer.

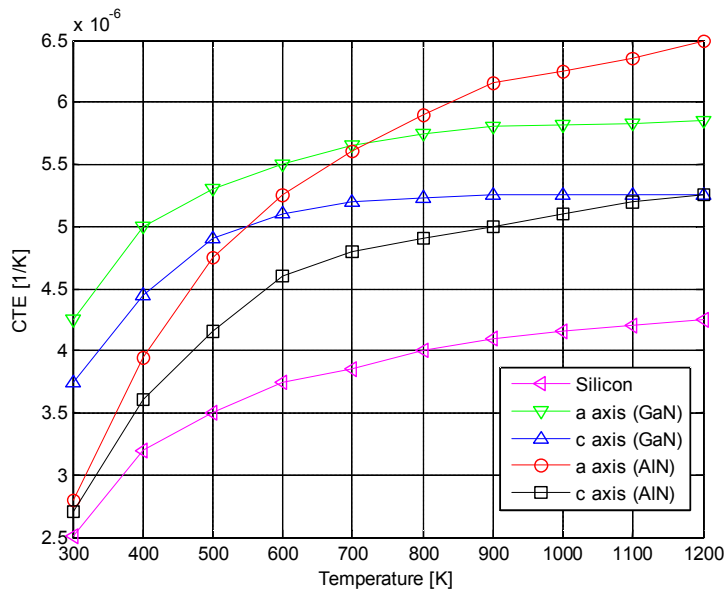
To perform it, the appropriate temperature ranges for the removal of the Si substrate must be considered. In a specific temperature range, the stress in the GaN layer grown on a Si substrate will be compressive or, ideally, zero

instead of tensile. If Si can be eliminated completely in the temperature range at which the GaN was grown on the Si substrate, it will be possible to fabricate a freestanding GaN without any stress evolution. The other contributing factor, the elastic stress (σ_{EL}), can be decreased by using an AlN buffer layer, which can reduce the lattice mismatch between GaN and Si.^{9,10)} In addition, an AlN buffer layer also prevents the out-diffusion of Si from the substrate into the GaN layer.¹¹⁾

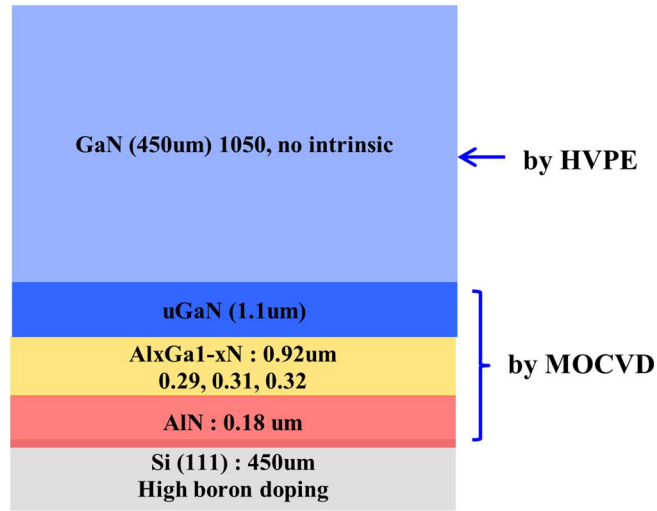
To evaluate the optimum temperature required for the removal of the Si substrate, the stress distribution (or bowing values) as a function of temperature in the GaN layer grown on a Si substrate was simulated using the finite element method (ABAQUS). The mechanical properties such as Young's modulus, Poisson's ratio, and coefficient of thermal expansion are detailed in Table 4-1 and Fig. 4-3. In addition, the thick GaN/MOCVD buffer layers/Si substrate structure to be realized at high temperature is characterized in Fig.4-3(b).

	Si (111)	GaN
Young's Modulus (MPa)	130000	297000
Poisson's ratio	0.263	0.25
CTE	α (T)	α (T)

Table 4-1. Mechanical properties of Si (111) and GaN used in numerical analysis



(a)

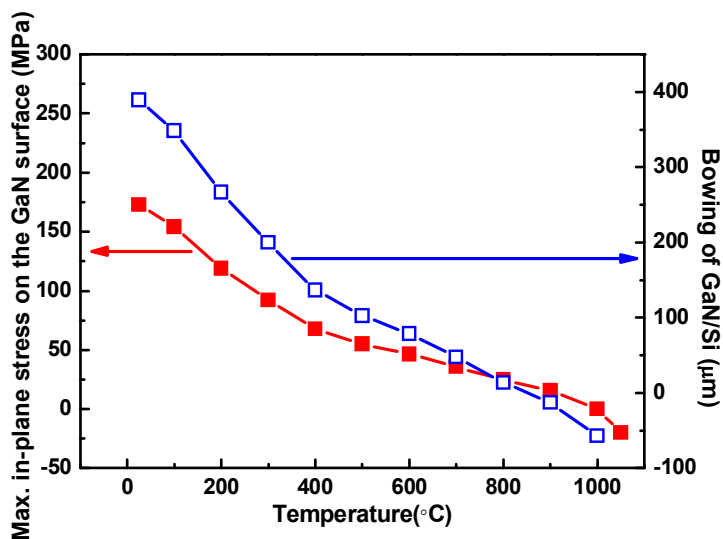


(b)

Figure 4-3. (a) CTE of Si and GaN along axis vs temperature, and (b) Schematics of layer structure applied in numerical analysis. The intrinsic stress at growth temperature was substituted by -679, and 20 MPa in MOCVD-uGaN and HVPE-GaN, respectively.

Figure 4-4 shows the numerical analysis for the temperature dependence of the in-plane stress and bowing in a thick GaN layer of 450 μm in thickness grown on a Si substrate of the same thickness. Considering the structure of MOCVD buffer layer on Si substrate, compressive stress is applied to HVPE GaN layer intrinsically at growth temperature. When calculating its value by

-20 MPa, the stress was changed from compressive stress to stress-free at 1000 °C after HVPE GaN growth. Tensile stress was increased with decreasing temperature during cooling of HVPE reactor. In other words, the nature of stress induced in the thick GaN layer grown on a Si substrate is tensile in the range from room temperature to 900 °C, but changes from tensile to compressive at 1000 °C. This theoretical prediction strongly suggests that the approach proposed in this study can be successfully implemented. The analysis for bowing of GaN/Si structure corresponds to above statement.



(a)

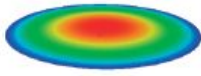
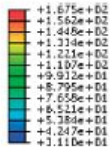
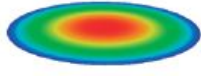
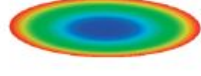
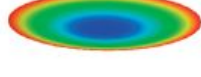
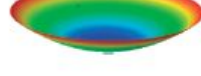
Temp (°C)	Max. in- plane Stress (MPa)	Bowing (μm)	Curvature shape		Type of stress in GaN layer
1000	-0.07	-57.3			compressive
900	15.5	-13.2			tensile
600	46.2	78.5			tensile
400	67.5	136.4			tensile
25	172.9	389.6			tensile

Figure 4-4. (a) The numerical analysis for temperature dependence of stress in a thick GaN layer grown on Si substrate. (b) The numerical analysis for temperature dependence of stress and bowing in GaN grown on Si substrate.

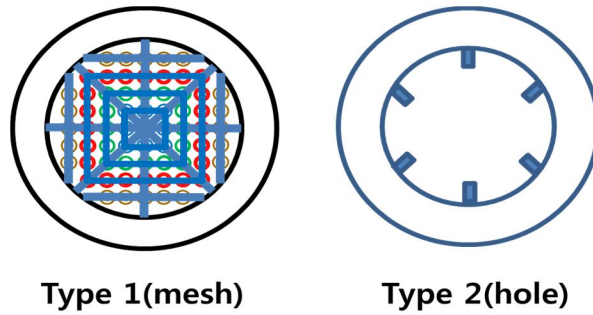
Furthermore, this calculation has it that crack in tensile stress state can be evolved at a third of compress stress state, thus implying that freestanding GaN can be obtained from Si substrates if Si substrates will not be removed above 700 °C after HVPE GaN growth.

4.3.3. Effects on gas flow rate and susceptor design for the etch of Si substrate

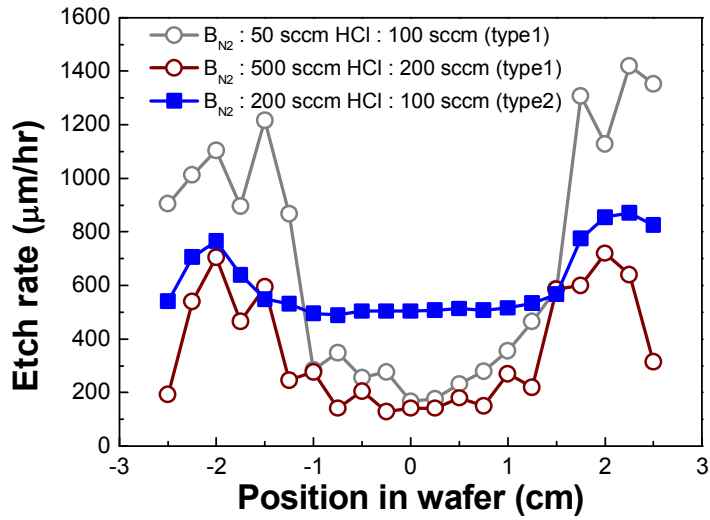
The uniformity of Si substrate is one of the most important factors to obtain freestanding GaN using in-situ removal of substrate. To perform completely and uniform etching of Si substrates, rotative susceptors with varying shape were constructed and applied.

Figure 4-5 shows the etch rate of Si substrates as a function of susceptor

shape and gas flow rate. It is noticeable that susceptor type 2 with larger contact area of Si substrates for HCl gas flow has better uniformity than susceptor type1. Moreover, the ratio of HCl and N_2 can decide the etch uniformity as shown in Fig 4-5(b) with varying etch rate deviation within Si wafers.



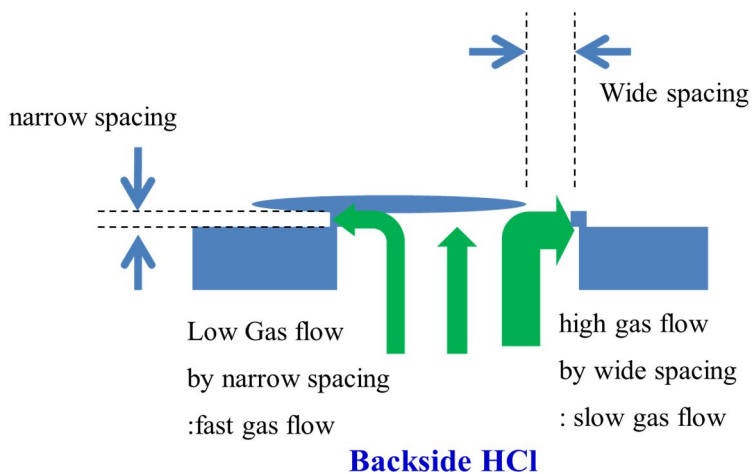
(a)



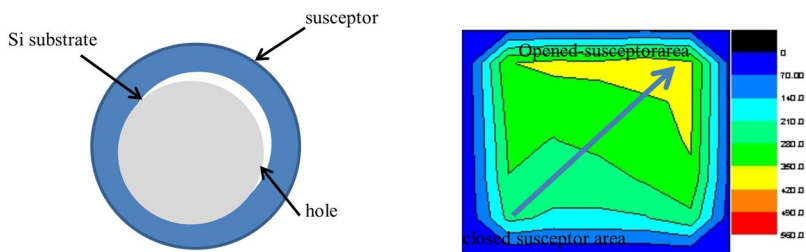
(b)

Figure 4-5. (a) Susceptor type used in the etch of Si substrate, and (b) etch rate of Si substrate as a function of susceptor types and gas flow rate.

Indeed, the position of Si substrate in susceptor need to be considered, when checking the etch rate uniformity of Si substrate. biased position of Si substrate on susceptor can make HCl gas flow deviation, resulting in etch rate difference as shown in Fig. 4-6. Note that wide spacing between Si substrate and susceptor leads the high etch rate of Si substrate in Fig. 4-6(b).



(a)

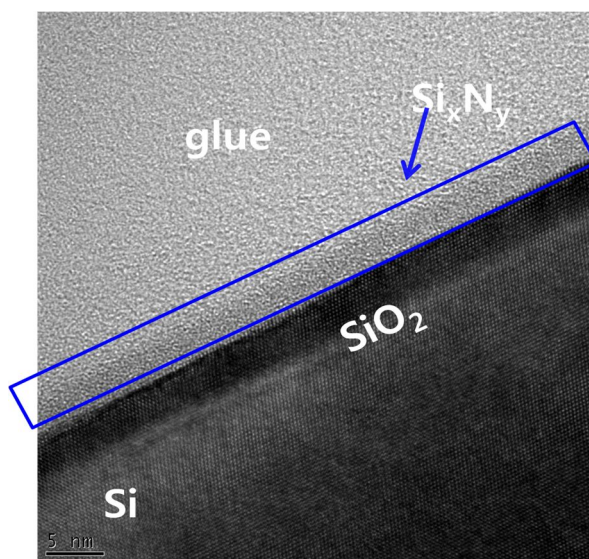


(b)

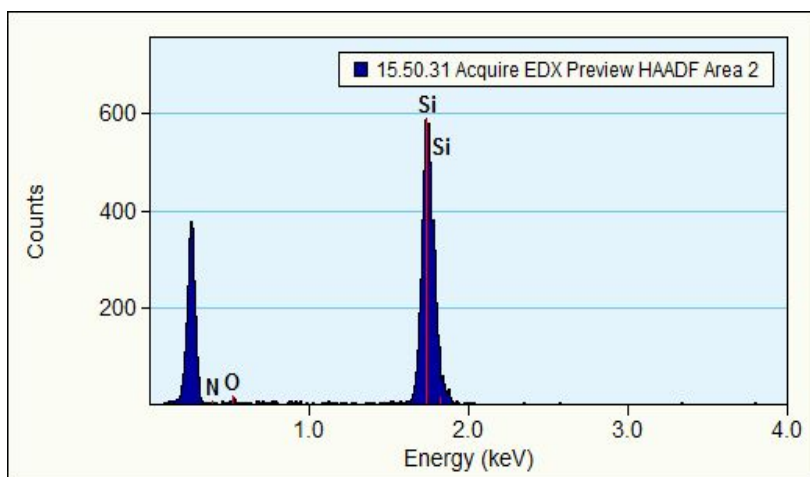
Figure 4-6. (a) Loading position of a Si substrate on susceptor vs HCl flow rate, and (b) etch rate of a Si substrate.

Unintentional and non uniform Si_xN_y deposition on the backside of Si

substrates prevent the uniform etch of Si substrate, in which Si_xN_y was formed by reaction between the back stream of NH_3 gas for GaN growth and Si substrate. Figure 4-7 depicts that cross sectional TEM image on backside of Si substrate after growing HVPE GaN and then etching Si substrate sequentially in HVPE reactor, which means the formation of Si_xN_y on the backside of a Si substrate were occurred during in-situ etch process. Energy dispersive X-ray spectroscopy (EDS) confirmed the formation of Si_xN_y where the phase and thickness were amorphous and 3-4 nm in thickness, respectively.



(a)



(b)

Figure 4-7. (a) Cross sectional transmission electron microscopy image of the backside on a Si substrate after etching Si substrate in HVPE reactor. (b) EDS data on backside of a Si substrate after growing GaN and then applying in-situ etch of Si substrate in HVPE reactor.

In case of bare Si substrates with 400 in thickness can be etched within 60 min completely. Si substrates with unintentional Si₃N₄ deposition, however, were etched in 150 min completely. To improve it, we had to consider some factors such as etching temperature and backside N₂ flow rate.

4.3.4. Meltback effect as a function of MOCVD buffer layer

To prevent the meltback effects in freestanding GaN, the thickness of MOCVD buffer layers was varied as shown in Fig. 4-8.

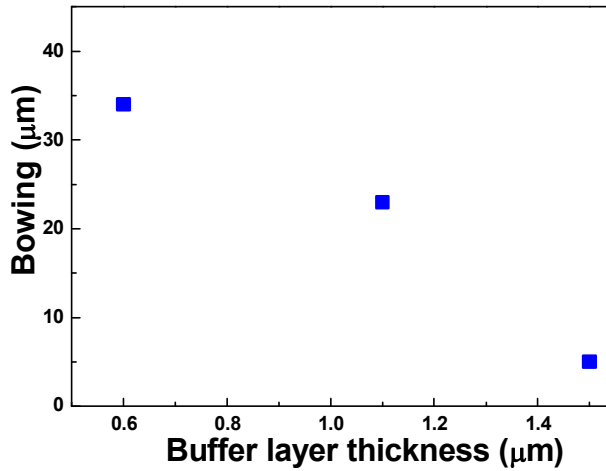


Figure 4-8. MOCVD buffer layer thickness vs bowing of MOCVD buffer layer/Si templates.

Note that the value of bowing in MOCVD buffer layer/Si templates decreases with increasing MOCVD buffer layer thickness, implying the increase in the compressive stress in MOCVD buffer layers. The accumulation of compressive stress in MOCVD buffer layers by increasing

the thickness of MOCVD buffer layers can compensate the increment of tensile stress in growing HVPE GaN. Indeed, the results correspond to above statements. When using MOCVD buffer layer with 0.6 μm in thickness, freestanding GaN always had meltback area. In case of a freestanding GaN grown on MOCVD buffer layer with 1.0 μm in thickness, meltback effect could be kept back despite of the crystal quality degradation of HVPE GaN. freestanding GaN without meltback, however, could be obtained using MOCVD buffer layer with 1.5 μm in thickness.

4.3.5. The properties of freestanding GaN grown from Si substrate

Figure 4-9 shows a photograph of the fabricated freestanding GaN. Figure 4-9(b) and (c) show surface and cross-sectional optical microscopic images of a freestanding GaN after the removal of a Si substrate, respectively. It can clearly be seen that the freestanding GaN was 400 μm in thickness and without any cracks or observable defects such as meltback and pits. Also, MOCVD buffer layers were completely etched, confirmed by SEM analysis (not shown in Figure)

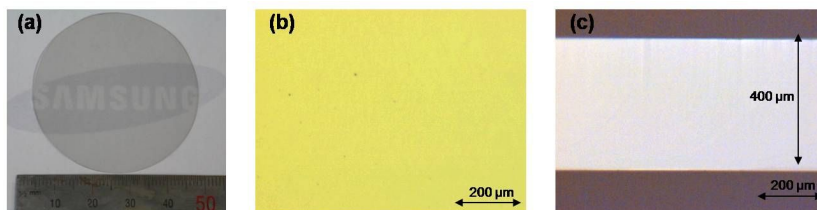
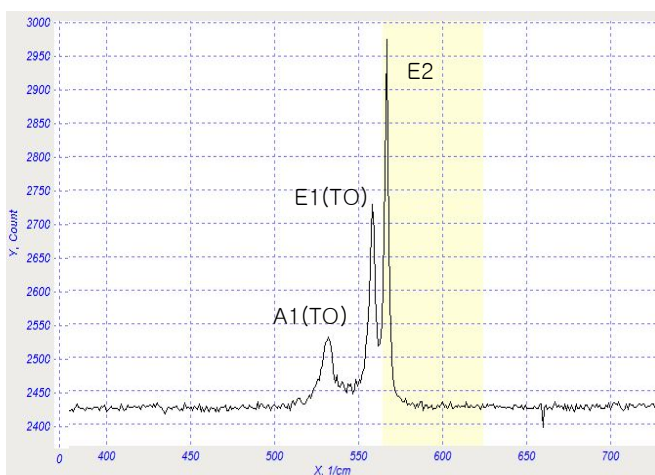
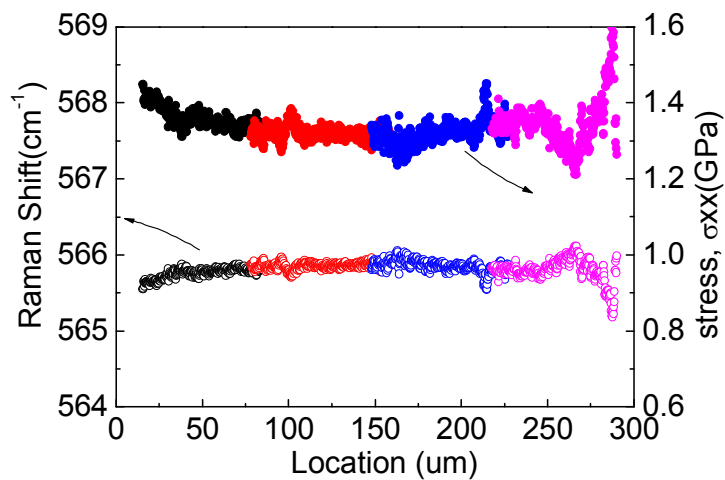


Figure 4-9. (a) Photograph of the freestanding GaN of 400 μm in thickness and with a diameter of about 2 inches. (b) Surface image of the freestanding GaN obtained using an optical microscope. (c) Cross-sectional microscopic image of the freestanding GaN ($\times 400$).

Typical stress profile of GaN layer was studied by micro Raman spectroscopy measurements at room temperature as demonstrated in Fig. 4-10. A_1 (TO), E_1 (TO) and E_2 (high) phonon modes can be identified with 531.3, 558.1 and 566.2 cm^{-1} , respectively as shown in Fig 4-10(a). The modes frequencies in measured Raman spectra are comparable with typical values for that of strain-free bulk GaN with 569 cm^{-1} .



(a)



(b)

Figure 4-10. (a) Micro Raman scattering spectra of a freestanding GaN

wafer and (b) micro Raman intensity profiles for E_2 (high).

We can easily notice that E_2 mode frequency has the red-shift, indicating the residual tensile stress about 200 MPa in a freestanding GaN wafer.

In order to determine a strain distribution in freestanding GaN substrate as a function of thickness, micro Raman scattering spectra from an edge of a cross-section (x(z)y)x geometry) were measured as depicted in Fig. 4-10(b). Note that micro Raman intensity for E_2 phonon mode is fairly uniform distribution, which is indicative of no stress evolution during HVPE GaN growth.

Figure 4-11(a) shows the (0002) X-ray rocking curve of the freestanding GaN. The FWHM for the diffraction peak was found to be 65 arcsec for the Ga-faced freestanding GaN, and 200 arcsec for the N-faced one. This small difference in FWHM between Ga- and N-face of freestanding GaN influences on the value of bowing for it. Typical bowing values of as-grown freestanding GaN from foreign substrates are more than a few hundred micrometers. Meanwhile, the bowing value of as-grown freestanding GaN

grown on Si wafer using in situ removal of substrate was below 20 μm of concave shape. This results from the absence of tensile stress evolution during cooling after growth of GaN and small difference of crystal quality between Ga and N-face in freestanding GaN grown on MOCVD GaN. We consider that the small difference in crystal quality between Ga- and N-face of freestanding GaN results from the matching of crystal quality between N-faced of HVPE GaN and MOCVD GaN grown on Si substrate. When considering the effects of MOCVD GaN layer for the bowing, if MOCVD GaN layer remains after the etch, it can increase the bow value in freestanding GaN due to large crystal quality difference between Ga-face GaN in HVPE GaN and N-face GaN in MOCVD GaN. MOCVD GaN layer, however, was completely etched so that its effects on the bowing were negligible. According to Fujikura et al¹²⁾, IDs, usually found in the bottom of pits, can decrease the stress and the bow of freestanding GaN. As-grown freestanding GaN from Si substrate, however, had very low density of pits on the surface. Therefore, we expect that the low bow value in freestanding GaN grown on Si substrate is not influenced on the IDs.

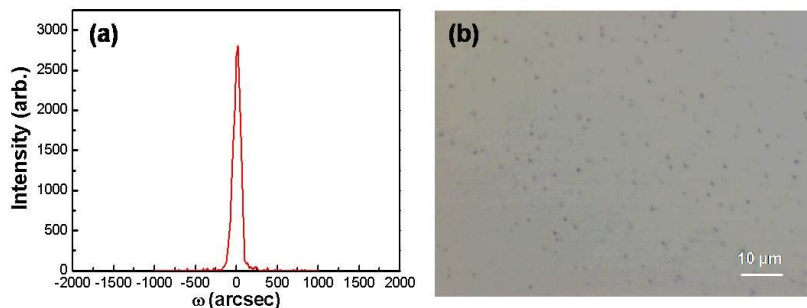


Figure 4-11. (a) (0002) X-ray rocking curve of the freestanding GaN. (b) Microscopic image of the freestanding GaN after H_3PO_4 etching at 200 °C for 30 min.

Moreover, the crystal quality was confirmed by measuring the EPD after etching the freestanding GaN in a H_3PO_4 solution at 200 °C for 30 min, as shown in Fig. 4-11(b). The estimated EPD was less than $1 \times 10^6 / \text{cm}^2$ over the whole wafer surface. These values are comparable to or even better than those of GaN layers grown on sapphire substrates reported elsewhere.¹³⁻¹⁵⁾ Therefore, even though the thickness of the freestanding GaN grown on the Si substrate is only 400 μm , its crystal quality is comparable to that of thick HVPE GaN with a thickness of over 1 mm.^{16, 17)}

Figure 4-12 shows 10 K PL spectrum of the freestanding 400 μm thick

GaN. The edge peak position of this PL spectrum is close to that for freestanding GaN grown on sapphire.^{18,19)} The spectral lines indicate a high optical quality of the freestanding GaN, as confirmed by the presence of the well-resolved free-excitonic line (FX) at 3.47 eV and the neutral donor bound-exciton (DBE) transition (D^0-X) at 3.467 eV with a FWHM value of 3.1 meV.^{20,21)} These results also confirm the high crystal quality of the freestanding GaN, as revealed by X-ray rocking curve and EPD measurements. The energy position of the DBE peak of the freestanding GaN was red shifted compared to that of strain-free GaN grown using the ammonothermal method or homoepitaxy (3.471 eV), implying that tensile stress is slightly present in the freestanding GaN.^{22–24)} Typically, when GaN layers are grown on an AlN/Si substrate, the compressive stress tends to accumulate in the GaN layers, and GaN layers grown on a Si substrate suffer from tensile stress caused by $\epsilon_{TH(RT)}$ during cooling after the growth of GaN. However, after the etching of the Si substrate, the GaN layers do not undergo tensile stress but retain a little bit of compressive stress incurred during the cooling phase due to the absence of $\epsilon_{TH(RT)}$. Therefore, this red shift can be attributed to the residual strain due to the quality difference for Ga- and N-face surfaces of the freestanding GaN grown on the Si substrate.²⁵⁾

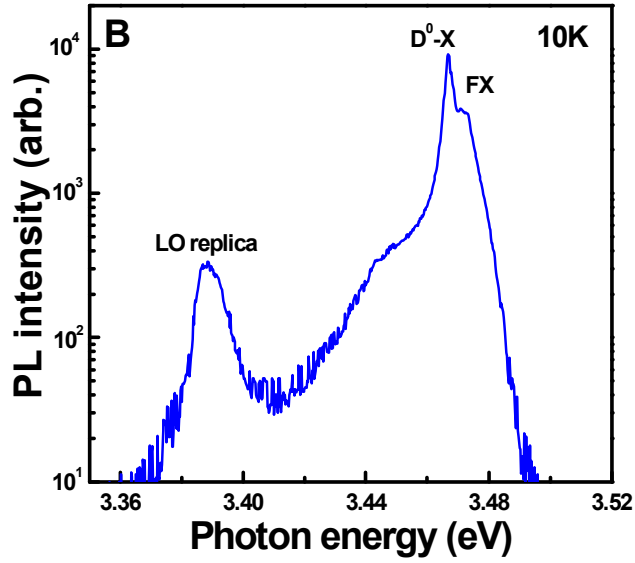


Figure 4-12. PL spectrum of freestanding GaN at 10 K.

4.4. Summary and Conclusions

In conclusion, high crystal quality freestanding HVPE GaN of 400 μm in thickness and 2 inches in diameter was successfully obtained by in-situ removal of Si substrate. The FWHM of (0002) x-ray rocking curve was estimated as 65 arcsec and the EPD was less than $1 \times 10^6/\text{cm}^2$, confirming the high crystal quality of freestanding GaN grown by this technique. The removal of Si substrate at high temperature can provide a practical way to

obtain freestanding GaN of high crystal quality from Si substrate. This approach is the promising way to get the high crystal quality freestanding GaN over 8 inches in diameter readily and economically.²⁶

References

- [1] S. Nakamura, M. Senoh, and T. Mukai, 1993, *Appl. Phys. Lett.* **62**, 2390
- [2] I. Martil, E. Redondo, and A. Ojeda. 1997, *J. Appl. Phys.* **81**, 2442
- [3] M. K. Kelly, R. P. Vaudo, V. M. Phanse, L. Gorgens, O. Ambacher, and M. Stutzmann, 1999, *Jpn. J. Appl. Phys. Part 2* **38**, L217
- [4] R. Armitage, Qing Yang, H. Feick, J. Gebauer, and E. R. Weber, 2002, *Appl. Phys. Lett.* **81**, 1450
- [5] A. Able, W. Wegscheider, K. Engl, and J. Zweck, 2005, *J. Cryst. Growth*, **276**, 415
- [6] T. H. Yang, J. T. Ku, J. Chang, S. Shen, Y. Chen, Y. Y. Wong, W. C. Chou, C. Chen, and C. Chang, 2009, *J. Cryst. Growth.* **311**, 1997
- [7] H. Ishikawa, G. Y. Zhao, N. Nakada, T. Egawa, T. Jimbo, and M. Umeno, 1999, *Jpn. J. Appl. Phys.* **38**, L492
- [8] E. V. Etzkorn and D. R. Clarke, 2001, *J. Appl. Phys.* **89**, 1025
- [9] M. Iwaya, T. Takeuchi, S. Yamaguchi, C. Wetzel, H. Amano, and I.

Akasaki, 1998, *Jpn. J. Appl. Phys.* **37**, L316

[10] A. Dadgar, J. Bläsing, A. Diez, A. Alam, M. Heuken, and A. Krost, 2000, *Jpn. J. Appl. Phys.* **39**, L1183

[11] A. Krost, A. Dadgar, J. Blasing, A. Diez, T. Hempel, S. Petzold, J. Christen, and R. Clos, 2004, *Appl. Phys. Lett.* **85**, 3441

[12] H. Fujikura, Y. Oshima, T. Megro, and T. Saito, 2012, *J. Cryst. Growth.* **250**, 38

[13] W. Luo, J. Wu, J. Goldsmith, Y. Du, T. Yu, Z. Yang, and G. Zhang, 2012, *J. Cryst. Growth.* **640**, 16.

[14] C. L. Chao, C. H. Chiu, Y. J. Lee, H. C. Kuo, P.-C. Liu, J. D. Tsay, and S. J. Cheng, 2009, *Appl. Phys. Lett.* **95**, 051905.

[15] D. Gogova, C. Hemmingsson, B. Monemar, E. Talik, M. Kruczek, F. Tuomisto, and K. Saarinen, 2005, *J. Phys. D: Appl. Phys.* **38**, 2332.

[16] D. Hanser, M. Tutor, E. Preble, M. Williams, X. Xu, D. Tsvetkov, and L. Liu, 2007, *J. Cryst. Growth.* **305**, 372.

[17] H. Geng, H. Sunakawa, N. Sumi, K. Yamamoto, A. A. Yamaguchi, A. Usui, 2012, *J. Cryst. Growth.* **350**, 44.

- [18] S. T. Kim, Y. J. Kim, D. C. Moon, C. H. Hong, and T. K. Yoo, 1998, *J. Cryst. Growth.* **194**, 37.
- [19] H. J. Lee, S. W. Lee, H. Goto, S. H. Lee, H. J. Lee, J. S. Ha, T. Goto, M. W. Choi, T. Yao, and S. K. Hong, 2007, *Appl. Phys. Lett.* **91**, 192108.
- [20] D. Y. Song, M. Basavaraj, S. A. Nikishin, M. Holtz, V. Soukhoveev, A. Usikov, V. Dmitriev, 2006, *J. Appl. Phys.* **100**, 113504.
- [21] G. Pozina, C. Hemmingsson, J. P. Bergman, D. Trinh, L. Hultman, B. Monemar, 2007, *Appl. Phys. Lett.* **90**, 221904.
- [22] J. Bai, M. Dudley, B. Raghathamachar, P. Gouma, B. J. Skromme, L. Chen, P. J. Hartlieb, E. Michaels, J. W. Kolis, 2004, *Appl. Phys. Lett.* **84**, 3289.
- [23] N. Y. Garces, B. N. Feigelson, J. A. Freitas Jr., J. Kim, R. L. Myers-Ward, E. R. Glaser, 2010, *J. Cryst. Growth.* **312**, 2558.
- [24] B. J. Skromme, K. C. Palle, C. D. Poweleit, H. Yamane, M. Aoki, and F. J. DiSalvo, 2002, *Appl. Phys. Lett.* **81**, 3765.
- [25] S. S. Park, I. W. Park, and S. H. Choh, 2000, *J. Appl. Phys.* **39**, L1141.

[26] M Lee, D. Mikulik, J. Kim, Y. Tak, J. Kim, M. Shim, Y. Park, U. Chung, E. Yoon, and S. Park, 2013, *Appl. Phys. Express.* **6**, 125502

CHAPTER 5.

Summary and Conclusions

In summary, the following contributions were made through this dissertation;

Chapter 2 provides details for the growth of GaN on sapphire substrate with 4 inch diameters in HVPE where AlN and GaN dot nuclei buffer layer acting as stress relaxation buffer layer was on the pages. by forming AlN/GaN nano dots on sapphire substrate, a 400 μm thick GaN was grown on sapphire substrates with 4 inch diameters. The thickness of stress relaxation layer was determined by the density and average size of AlN/GaN nano dots. The larger size and the less density nano dots, the slower coalescence of nano dots, making stress relaxation layer thicker. Growth parameters such as pretreatment temperature, NH_3 gas flow rate, HCl flow rate could control the density and average size of AlN/GaN nano dots. To make uniform gas flow stream in HVPE reactor, we designed new gas nozzle with tripod shape where GaCl gas flow could be delivered uniformly at proper distance (in 60 mm distance from nozzle to susceptor). Finally, a 400 μm thick GaN was grown on sapphire substrate with 4 inch in diameters. The value of FWHM in (0 0 0 2) X-ray rocking curve of a thick GaN was 220 arcsec. After lift-off of sapphire substrate, FWHM obtained for (0 0 0 2) reflection were 123 arcsec, which the bowing of wafer was changed from convex to concave, implying the tensile stress. In addition, via etch pit

density measurement the crystal quality of freestanding GaN grown on sapphire substrate was confirmed. EPD density was about $5 \times 10^6/\text{cm}^2$. Photoluminescence analysis present the optical property of freestanding GaN grown on sapphire substrates. The band edge peak was on 3.393 eV which was moved to red-shift by about 78 meV compared to strain-free bulk GaN, indicating tensile stress in GaN layers.

In chapter 3, the homoepitaxial bulk GaN growth was detailed. For freestanding GaN with extremely low defect density below $10^4/\text{cm}^2$, the unique approach was used for the growth of GaN on GaN substrates where substrates was pre-treated by pit-assisted growth. The pit-assisted growth method of GaN was employed by intentional formation of etch pit on the Ga-face of freestanding GaN. To perform it, freestanding GaN substrate was handled by HCl gas treatment at 900 °C in HVPE reactor, and subsequently dipped into H_3PO_4 acid solution at 200 °C during 30 min. The etch pits generated by intentional pit formation, is composed of three kinds of types: α -type etch pit - an inverse-truncated hexagonal pit, the β type one - an inverse-hexagonal pyramid, and the last γ type one - a trapezoidal type. Each etch pit types are related to the screw, edge, and mixed dislocation, respectively. Similarly to the results from other freestanding GaN, most of etch pits consists of β type etch pit, originating from the edge dislocations.

This means that screw dislocations are readily annihilated by increasing the thickness of GaN. By applying pit-assisted growth method, bulk GaN with 5 mm in thickness, and 3 inch in size, respectively was grown. The surface of bulk GaN is relatively plain, and transparent. FWHM of X-ray rocking curve at (0 0 0 2) diffraction was 28 arcsec, and the value of EPD was evaluated by $3 \times 10^2/\text{cm}^2$, indicating very extremely high crystal quality.

In chapter 4, high crystal quality freestanding HVPE GaN of 400 μm in thickness and 2 inches in diameter was successfully obtained by in-situ removal of Si substrate. The FWHM of (0002) x-ray rocking curve was estimated as 65 arcsec and the EPD was less than $1 \times 10^6/\text{cm}^2$, confirming the high crystal quality of freestanding GaN grown by this technique. The removal of Si substrate at high temperature can provide a practical way to obtain freestanding GaN of high crystal quality from Si substrate. This approach is the promising way to get the high crystal quality freestanding GaN over 8 inches in diameter readily and economically.

Abstract (in Korean)

갈륨나이트라이드(GaN)는 넓은 밴드갭, 높은 열전도율과 항복 전압 등의 고유의 물리적 특성으로 인하여 광전자 소자 및 고주파수 전자 소자 등을 위한 재료로 각광받고 있다. 갈륨나이트라이드는 자연계에 존재하지 않기 때문에 화학 기상 증착법, 분자선증착법이나 HVPE 등 이종 성장 방법을 통하여 이종 기판에 성장하여 얻고 있다. 그러나, 이종 기판에 성장된 갈륨나이트라이드는 갈륨나이트라이드와 이종 기판 계면 사이에서 발생한 높은 전위 밀도로 인하여 광전자 소자에의 응용이 제한적이다. 갈륨나이트라이드 기판을 사용하여 소자를 형성할 경우 높은 전위 밀도로 인한 소자 특성 저하를 개선할 수 있지만, 이를 실현하기 위해서는 몇 가지 넘어야 할 문제들이 있다. 첫째로는, 비교적 높은 전위 밀도이다. 일반적으로

갈륨나이트라이드 기판은 $10^6/\text{cm}^2$ 수준의 전위 밀도를 갖지만 이러한 수치는 특정한 파장의 레이저 다이오드나 파워 디바이스에는 충분치 못한 수준으로 간주된다. 두 번째는 기판 크기의 한계와 제작 비용적인 측면이다. 이를 실현하기 위해서는 기판 크기와 비용, 그리고 결정 구조를 만족시키는 이중 기판이 필요하다. 갈륨아스나이드 기판의 경우에 기판의 가격이 너무 비싸 저가격 갈륨나이트라이드 기판을 제작하는데 적합하지 않다. 또한, 사파이어 기판의 경우 기판 크기의 한계로 인하여 대구경의 갈륨나이트라이드 기판을 만드는데 부적합하다.

본 학위 논문에서는 위 문제를 해결하고자 HVPE 법으로 몇 가지 특수한 방법을 통하여 갈륨나이트라이드 기판을 성장하는 방법에 대해 논의하고자 한다.

첫 번째로, 갈륨나이트라이드 나노 점(Nano dot)을 이용한 스트레스 완충 층(stress relaxation layer)을 통해 사파이어 기판 상에

갈륨나이트라이드를 성장하여 4 인치 freestanding 갈륨나이트라이드 기판을 제작하는 방법을 제시하였다. 이 방법을 통하여 두께 400 마이크로미터와 4 인치 크기를 갖는 freestanding 갈륨나이트라이드 기판을 제작하는데 성공하였다. 이 때, 사파이어 기판 상 갈륨나이트라이드의 결정성은 X-ray 회절 분석의 반치폭(FWHM)으로 분석되었을 때 220 arcsec 였으며, 사파이어 기판을 떼어냈을 때, 123 arcsec 로 향상되는 것을 확인하였다. 기판의 힘은 사파이어 기판이 존재할 경우 블록한 상태에서, 떼어냈을 때 오목한 형태로 바뀌었다. 갈륨나이트라이드 기판의 결정성은 etch pit 밀도를 통해서도 확인되었는데 $5 \times 10^6/\text{cm}^2$ 수준이었다. 기판의 광학적 특성은 광발광 분광법 (Photoluminescence)을 이용하여 확인되었으며 edge peak 가 3.393 eV 에 위치한 것으로 보아 기판에 스트레스가 존재하지 않는 bulk

GaN 와 비교하였을 때, 78 meV red-shift 특성을 나타내었다. 이는

갈륨나이트라이드 층에 인장 응력이 존재함을 보여주는 결과이다.

다음으로, homoepitaxy 성장에 의해 초저결함 밀도를 갖는 bulk 갈륨나이트라이드를 성장하는 방법에 대해 논의할 것이다.

HVPE 반응로 내에서 HCl 가스로 처리된 갈륨나이트라이드 기판을

인산 식각 처리를 통하여 etch pit 밀도를 증가시켰다. 이렇게 etch

pit 밀도가 증가된 갈륨나이트라이드 기판을 이용하여

갈륨나이트라이드를 성장하였으며, 매 1 mm 두께마다 이러한

기판에 대한 식각 처리가 행해졌다. 이 성장법을 pit-assited

성장이라고 명명하였다. Etch pit의 형태는 3 가지 형태로 나타났는데

α type 은 끝이 잘려진 역 육각피라미드 형태, β type 은

역육각피라미드 형태, 마지막으로, γ type 은 사다리꼴 형태의

형태였으며, 이 들은 각 각 screw, edge, mixed 전위가 그 기원이었다.

기 성장되어왔던 갈륨나이트라이드 기판의 결과들과 마찬가지로,

etch pit 의 대부분이 β 형태의 etch pit 이었다. 최종적으로 5 mm 두께와 3 인치 크기를 갖는 갈륨나이트라이드가 성장되었으며 etch pit 밀도는 $3 \times 10^2/\text{cm}^2$ 수준이었다.

마지막 장에서는, Si 기판으로부터 갈륨나이트라이드 기판을 제조하는 방법에 대해 논의하고자 한다. 지금까지, 갈륨나이트라이드 기판은 인장 응력 생성과 meltback 문제로 인하여 Si 기판으로부터 성장하는 것이 불가능했었다. 그러나, 이 장에서 제시하는 기판 in-situ 제거법이라는 독특한 방법을 이용하였을 때 갈륨나이트라이드 기판을 Si 기판으로부터 성장하는 것이 가능하였다. 즉, 갈륨나이트라이드 성장 후 반응로 온도 하강 시 나타나는 인장 응력을 제거하기 위하여 Si 기판은 성장 온도에서 HCl 가스에 의해 식각되었고, 이를 통해 인장 응력의 생성은 완전히 제거되었다. 이를 통해 400 마이크로미터 두께와 2 인치 크기를 갖는 갈륨나이트라이드 기판이 Si 기판으로부터 성장되었다.

이 때 X-ray 회절에 의한 반치폭 값은 65 arcsec 이었으며, etch pit 밀도는 $1 \times 10^6 / \text{cm}^2$ 수준이었다. 이 방법을 이용한다면 고결정질의 8 인치 크기 이상의 대구경 갈륨나이트라이드 기판을 제조하는 것이 가능할 것이다.

Key words: 갈륨나이트라이드(GaN), freestanding 갈륨나이트라이드, HVPE, 전위, 스트레스 완충층, 나노점, etch pit, 광발광 분광법 (photoluminescence), bulk 갈륨나이트라이드, pit-assisted 성장, in-situ 제거

학번: 2011-30937